Simulation and Control of Submarines

Erik Lind

Magnus Meijer

LUND UNIVERSITY

Department of Automatic Control

MSc Thesis
ISRN LUTFD2/TFRT--5954--SE
ISSN 0280-5316

Department of Automatic Control
Lund University
Box 118
SE-221 00 LUND
Sweden

Printed in Sweden by Media-Tryck
Lund 2014

Abstract

When designing control systems for real applications, it is important to first do testing in a simulated environment, to ensure adequate performance. This is especially important when designing control systems for applications that have high operation costs, e.g., submarines, since late errors in the development can be extremely costly.

Saab develops steering systems for submarines. Prior to this thesis, testing for those have been performed in an open-loop environment, where only static test cases could be examined. Saab therefore identified the need to implement a dynamic test simulator, which could react to the different signals from the steering system, i.e., act as a real submarine.

In this thesis, such a simulator was developed. It consists of two parts, a physical model of a submarine, and a control system for motion control. As for the physical submarine model, it can be approximated from mechanical data of a submarine that the user provide, such as dimensions and weight. The second options is for the user to explicitly supply the simulator with hydrodynamic coefficients.

The control system was derived to control a model of a demo submarine. Saab is also involved in submarine navigation systems and saw the need to, in the future, also have the possibility to test those products. A navigation system assumes an autopilot exists, hence, an autopilot control system was developed.

In the end, the control system consisted of a two-level cascade controller of mixed LQG- and PID-control, along with a Kalman estimator for estimating unknown states.

The results were overall satisfactory. The performance of the control system is well within usual customer specifications and the main problems in this thesis lay in getting a proper model.

Sammandrag

När styrsystem utvecklas för dyra applicationer, är det ofta viktigt att först uföra simulerade modelltester för att tidigt hitta fel och testa prestanda. På en ubåt är detta extra viktigt, eftersom fel som uppstår sent i utvecklingen kan bli väldigt kostsamma.

Saab utvecklar styrsystem till ubåtar. Innan detta examensarbete utfördes alla tester på dessa produkter i en statisk miljö, där en användare kunde skicka in insignaler till styrsystemet och studera utsignalerna från detta. Men användaren var själv tvungen att ändra på alla insignalerna för att studera ett annat fall. Saab såg därför behovet av en dynamisk simulator som kunde reagera på utsignalerna från styrsystemet, det vill säga, replikera en riktig ubåt.

I det här examensarbetet utvecklades en sådan simulator. Den består av två delar, en fysikalisk modell av en ubåt och en autopilot för att styra dess rörelser. För den fysikaliska modellen finns möjligheten att få en approximerad modell av en ubåt utifrån fysiska mått. Den andra möjligheten är att användaren förser simulatorn med alla hydrodynamiska koefficienter.

Autopiloten utvecklades att styra en demoubåt. Saab är också involverade i navigationssystem till ubåtar, och såg därför behovet av att i framtiden också kunna testa sådana produkter. Ett navigationssystem antar att det finns något som styr ubåtens rörelser, därför utvecklades också en autopilot.

Till slut bestod autopiloten av en kaskadregleringsdesign, där både LQG- och PID-reglering används, tillsammans med en Kalmanestimator för att skatta de okända tillstånden.

Resultaten var överlag goda. Prestandan på styrsystemet låg väl inom normala kundkrav, och de största problemen låg i att få fram en god modell.

Acknowledgements

The authors would like to offer our deepest gratitude to Saab Group for the opportunity to perform this thesis, and to get a valuable insight in engineering industry. Naturally, we would also like to thank Hans Bohlin at Saab who worked out the idea behind this master thesis, and has also been our supervisor at Saab. He has been a great mentor and has provided valuable help and assistance throughout this thesis.

Bo Carlsson assisted us with the implementation in C, this thesis would not have reached its final form without him.

We would also like to thank Mats Nordin and Lennart Bossér at FOI for the invitation to Stockholm. The meeting was very rewarding. Saab Underwater Systems also provided us with valuable tips and guidance, for which we are grateful for.

Finally, we would like to thank all the other nice people at Saab Support and Services for a pleasant time at Saab.

Erik Lind & Magnus Meijer
27/6 2014 Malmslätt, Linköping

Contents

List of Figures

List of Tables

Denominations

Table 0.1: List of variables

symbol	explanation	unit
δ	hydroplane mechanical angle	rad
δ_h	water inflow angle	rad
δ_e	$\delta - \delta_h$, effective rudder angle	rad
n	rotor RPS	/s
τ	torque	Nm
ρ	water density	kg/m^3
F	force	N
a	acceleration	m/s^2
x	position	m
v	velocity	m/s
ω	angular velocity	rad/s
$\mathbf{x}_G = (x_G, y_G, z_G)$	center of gravity	m
$\mathbf{x}_B = (x_B, y_B, z_B)$	center of buoyancy	m
O^A	origin of coordinate system A	-
ϕ	submarine roll	rad
θ	submarine pitch	rad
ψ	submarine yaw	rad
u	velocity submarine x direction	m/s
v	velocity submarine y direction	m/s
w	velocity submarine z direction	m/s
p	angular velocity about submarine x axis	rad/s
q	angular velocity about submarine y axis	rad/s
r	angular velocity about submarine z axis	rad/s
X	force component in submarine x direction	N
Y	force component in submarine y direction	N
Z	force component in submarine z direction	N
K	torque about the submarine x axis	Nm

M	torque about the submarine y axis	Nm
N	torque about the submarine z axis	Nm
W	gravity force	N
B	buoyancy force	N
ν_1	(u, v, w)	m/s
ν_2	(p, q, r)	rad/s
m	submarine mass	kg
L	submarine length	m
$\mathbf{I}$	submarine moment of inertia matrix	kg m^2
I_x	submarine moment of inertia about the x axis	kg m^2
I_y	submarine moment of inertia about the y axis	kg m^2
I_z	submarine moment of inertia about the z axis	kg m^2
I_{xy}	cross product, moment of inertia	kg m^2
I_{zx}	cross product, moment of inertia	kg m^2
I_{yz}	cross product, moment of inertia	kg m^2
$\mathbf{M}$	mass matrix	kg
C_d	drag coefficient	-
C_l	lift coefficient	-
$h(x)$	local height at position x	m
$b(x)$	local width at position x	m
$\mathbf{x}_{HPk}$	rudder k position	m
v_{rk}, V_{rk}	local water velocity at rudder k	m/s
v_{rek}, V_{rek}	projected water velocity at rudder k	m/s
L_{ru}	rudder lift force	N
D_{ru}	rudder drag force	N
Λ	rudder aspect ratio	-
$\mathbf{N}_k$	rudder k midline vector	-
$\mathbf{L}$	state feedback gain	-
$\mathbf{L}_r$	state feedforward gain	-
K_t	rotor force coefficient	-
K_q	rotor torque coefficient	-
D_p	rotor diameter	m
J	advance ratio	-

subscript	explanation
hs	hydrostatic
hd	hydrodynamic
p	propulsion
c	control
l	lift
d	drag

Table 0.2: List of subscripts

subscript/superscript	explanation	acronym
TG	gravity	G
B	buoyancy	B
W	water	W
R	reference	REF
L	earth	LL
HP_k	hydroplane k	HP_k

Table 0.3: List of coordinate systems

Abbreviation	Explanation
RPS	Revolutions Per Second
RPM	Revolutions Per Minute
INS	Inertial Navigation System
HP	hydroplane(s)
DOF	Degrees Of Freedom
SASS	Submarine Steering System
FF	Feed Forward
FB	Feedback
LQG	Linear Quadratic Gaussian
CFD	Computational Fluid Dynamics
CAD	Computer Aided Design
TCL	Tool Command Language

Table 0.4: List of abbreviations

1

Introduction

1.1 Submarines

Concepts of Military Submarines

Modern submarines are one of the most complex types of machines that exists today, only beaten by space shuttles. Submarines, i.e., underwater vehicles, come in many shapes, depending on if they are intended for underwater research, maintenance, or military purposes. This thesis will deal with the latter.

The historical intentions of military submarine are attacking enemy surface ships or other submarines. Today they also serve as portable missile launchers and their subtle nature, makes them suitable for surveillance and reconnaissance missions. Submarine are also used for deployment of special forces in enemy territory and other covert operations. All these advantages make submarines very popular for the world's military powers.

To properly serve these purposes, submarines naturally come with a number of desired features:

- ***Long operation endurance*** Submarines should be able to operate close to enemy borders, possibly far from own territory. Hence, long endurance is a very desirable feature since resupplying, e.g., from surfaced ships, could draw attention.

- ***Long submerged endurance*** The advantage with submarines over other military vessels, is the possibility to operate in stealth under water. Long underwater endurance is therefore a must. This have been an issue historically due to the crew's and combustion engines' need for oxygen.

- ***Low signature*** A submerged submarine can not be spotted by traditional means, e.g., radars. The historical way of finding submarines is instead by the sound they produce underwater, hence low noise levels are desired.

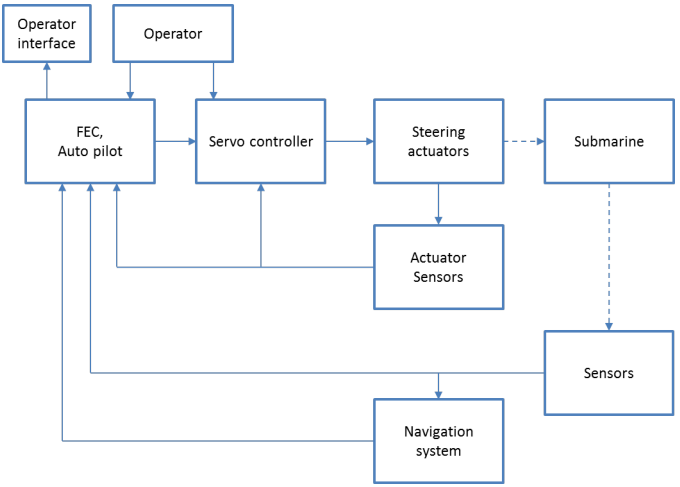

Figure 1.1: Submarine steering system.

Submarine steering system

Figure 1.1 shows a simplified structure of a submarine steering system and how it is integrated with other parts. Dashed lines are not signals, but rather physical feedbacks. The operator can chose between an autopilot, or manual steering. In the latter he/she could for example use a joystick/wheel to give references to the servo controller. To steer, the operator naturally needs the values from the different sensors displayed in some fashion (operator interface).

The navigation system is a device for high end navigation. A position could for example be given to the navigation system and it should generate a desired heading to reach the destination. Traditionally, the navigation system is a human navigator with a compass and sea charts.

The FEC (front end computer) handles the interface between the sensors and the operator displays. The servo loop serves as an inner loop to the actuators, improving the outer interface by allowing, i.e., rudder angles and propeller RPM[1] requests.

Steering actuators

In order to manoeuvre a submarine, a number of different steering actuators are needed. For a a surface going vessel, i.e., a boat, these could include the rudder and the propeller. A submarine typically also has additional steering actuators, some which will now be presented.

Sail The sail is not an actuator itself but will here be presented for future reference. The typical submarine hull consist of, in addition to the main hull, a so called tower

[1] Revolutions per minute

or sail. This serves as a centerboard that increases the submarines stability when manoeuvring through water. It is also the place for a number of masts and periscopes and usually also has a hatch for the crew.

Propeller A submarine is propelled forward by a propeller in the stern. For a submerged submarine, it is powered by a nuclear reactor in nuclear submarines or by a sterling engine, as in the Swedish submarines. The design of the propeller itself is quite complex and not seldom classified.

Bow propeller This is a propeller at the bow which creates a transverse propulsion and is used for docking at quay (this propeller will be excluded in this thesis).

Hydroplanes Water vehicles are steered with the means of rudders, submarines are no exception. The difference between submarines and surfaced vessels is that they have additional degrees of freedom (DOF). Traditional surface going ships include three means of control freedom, to steer (two DOF) and forward propulsion (one DOF). A submarine needs the ability steer in a upward/downward motion which adds additional two DOF. Most rudder configurations will also add roll as a control DOF.

All the different rudders and fins on submarines share the name hydroplane. A typical modern submarine includes 6 different hydroplanes, four in the stern and two at the bow or on the sail. When changing or keeping depth, this thesis will refer to two modes, the *sledge* and the *elevator*. The *sledge* mode is common in large depth changing manoeuvres and at higher speeds, while at lower speeds or in depth keeping situations, the *elevator* is preferred. They are both illustrated in Figure 1.2. There is also a tendency that in a middle velocity region, a combination of *sledge* and *elevator* manoeuvres are used.

When the hydroplanes are placed on the tower instead of at the bow, they can more or less alone be used to elevate the submarine. As they are located closer to the midship, i.e., closer to the center of the ship, the submarine will not suffer from the same kind of pitching movement as it would if the hydroplanes were placed at the bow. See Figure 1.3 for roll, pitch, and yaw definitions.

The stern hydroplanes are used as rudders and pitching fins. The classic configuration has been to place them as a + (Figure 1.4), with the lower vertical hydroplane slightly smaller to allow the submarine to move closer to the seabed. However, this will lead to a decreased manoeuvrability when surfaced. Another downside to the + configuration is that if one hydroplane has malfunctioned, the submarine will face considerable decreased manoeuvre performance in the direction the hydroplane was meant to work in. And in the case that two fins malfunction, there is the risk to completely lose manoeuvrability in a certain direction.

Another stern hydroplane configuration that is becoming popular on modern submarines is the $\times$- configuration (Figure 1.4). With this configuration every aft fin will create both horizontal and vertical force, which means they can all work together to create a yawing or pitching moment. It is then possible to manoeuvre

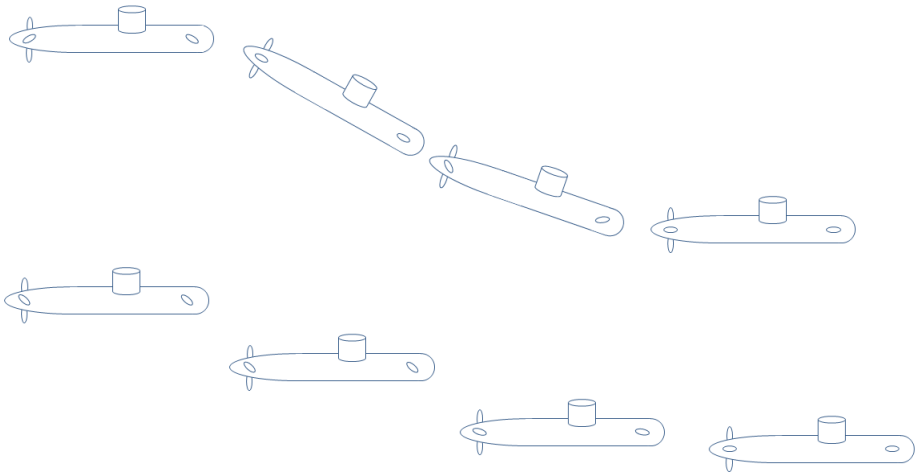

Figure 1.2: Submarine *sledge* and *elevator* movements.

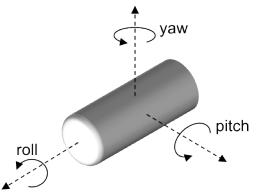

Figure 1.3: Roll pitch and yaw definitions.

well, even if two hydroplanes are out of service. And since they can all work together, they can be made smaller, which will decrease the drag force when moving forward. They will also be angled, which means the submarine can move closer to the seabed or quay without the hydroplanes getting in the way. The downside, however, is when in, for example, a yawing motion, one hydroplane will also create a pitching force that has to be cancelled by another hydroplane, which in turn will create unnecessary drag. Manoeuvring will also be more complex, i.e., it is less straight forward how to slant the hydroplanes to create the desired motion.

Tanks A submarine typically include four different types of water tanks:

- Ballast tanks
- Compensation tanks
- Trim tanks

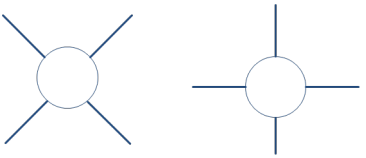

Figure 1.4: × and + rudder configuration.

- Balance tanks

The purpose of the *ballast tanks* is to make the submarine float or sink. These are typically huge and have just two modes, filled or empty. The *compensation tanks* are used to trim the weight so that the submerged submarine is weightless, i.e., hovers in the water. The *trim tanks* are basically one tank at the bow, and another in the stern, connected with a tube and a pump. Pumping water from one tank to another, moves the center of gravity, and can thus be used to make the submarine balanced in the water. The *balance tanks* are the same as the trim tanks, with the difference that they are instead used to achieve balance port relative starboard, rather then bow relative stern.

Sensors

Submerged submarines in northern waters have no means to with human eyes spot its surroundings due to the shallow water, even if a window would exist on the submarine which is rarely the case. A submarine must therefore include numerous sensors in order for an operator/autopilot to figure out what is going on. These sensors typically include:

- Log
- Depth sensor
- INS[2]
- GPS
- Water density sensor

Together, they measure:

- ***Attitude*** The current roll, pitch and heading, measured by the INS.
- ***Attitude rate*** Measure the current angular velocities of the magnitudes above. Also measured by the INS.

[2] Inertial navigation system

- ***World position*** Current longitude, latitude position, and the depth. The first two could be from a GPS system or from an INS. The GPS position is naturally more exact, but when submerged, the GPS will not be able to connect to satellites, hence, an INS is necessary. The depth is measured with, e.g., a pressure depth sensor.

- ***World velocities*** The velocities of the magnitudes above.

- ***Log velocities*** The current speed forward. Traditionally measured by log propellers/impellers, but modern submarines uses, e.g., pressure or acoustic logs.

- ***Current actuator state*** Naturally, it should possible to measure the current hydroplane angles and rotor RPM. In case of a, e.g., hydroplane malfunction, the operator or autopilot should notice if the hydroplane angle is not what it is set to be.

- ***Water density*** This is a vital measurement for the tank control, especially the compensation tank.

Manoeuvre a submarine

Historically, submerged submarine manoeuvring was performed by an officer giving commands to an operator, which angles to slant the different hydroplanes[3]. Modern techniques allows more sophisticated ways of manoeuvring. An operator, can today simply use a joystick to angle the hydroplanes. The joystick could more or less be directly connected to the hydroplanes, e.g., in the case of $\times$ rudder configuration, there is preferably a transformation between joystick movements and hydroplane angles to counter for the non straightforward nature of $\times$ rudder configuration manoeuvring.

Today's knowledge also allows for well performing autopilots. In this case, references could (and will, later in this thesis) be the desired depth, heading, and in some cases pitch.

1.2 Background

Submarine Steering System SASS

Saab develops steering systems for submarines. These steering systems typically includes autopilot computers, console for operator display, and control devices, interfacing to several steering actuators and steering and navigation sensors. Saab steering systems are currently used by submarines in Sweden, Australia, Norway, and Singapore. Saab is also involved in navigation system development.

[3] The reliability of this fact is the historical accuracy of the German film *Das Boot* from 1981.

1.3 Thesis concepts

TCL

TCL[4] is a very powerful but easy to learn dynamic programming language, suitable for a very wide range of uses, including web and desktop applications, networking, administration, testing and many more. Open source and business-friendly, TCL is a mature yet evolving language that is truly cross platform, easily deployed and highly extensible [*Tool Command Language*].

Matlab

The reader is assumed to have Matlab knowledge and experience, hence the program will not be extensively discussed here. In short, Matlab is a software developed by Mathworks, extensively used in the academic world and in industry to do mathematical calculations and simulations. [*Matlab*]

Simulink

Simulink is an extension to Matlab. It is a graphical programming tool often used to simulate dynamic systems and interconnection of multiple such. Matlab and Simulink were extensively used in the development of this thesis. [*Simulink*]

1.4 Scope of Master thesis

Purpose of the thesis

Submarines are generally very expensive in operation. As for a steering system, fault detection and controller autopilot tuning should therefore preferably be performed in advance, as far ahead of any real testing on-board as possible.

Prior to this thesis, the only means Saab have had for testing the steering system, before installation and on board test runs, were to simulate certain static cases with limited capability of verifying dynamic characteristics. The main part of the dynamic testing and verification had to be postponed to the end of the product development, when the system is installed in the submarine. In order to expand the means of testing, Saab therefore wanted to develop a simulator system, where hardware could be tested early in the production stage, thus minimizing the sea tests.

The purpose of this thesis is therefore to implement a submarine simulator, and thus make it possible to perform as much testing and tuning of new products as possible prior to target system implementation. This can be used for evaluating new hardware, tuning of autopilots or investigating how different sensor errors will affect performance.

[4] Tool Command Language

Thesis tasks and objectives

For a new product, it could be desirable to test the navigation system independently of the product's autopilot, hence the ability to test on an, already functional, autopilot should exist. Therefore, the simulator should consist of two separate parts, one submarine model and an autopilot to control the submarines movements.

From this point, the model simulator itself will be referred to as the *submarine simulator*. The autopilot part will be referred to as the *control system* or *autopilot* and them combined, submarine simulator together with the control system, as the *simulator system*. The *submarine model* will be the analytical model itself.

Submarine model The submarine model should naturally correspond to an actual full scale submarine as well as possible. It should include most of the hydrodynamic effects from the surrounding water and should at least include the rotor and the hydroplanes as actuators. All hydroplanes shall have the possibility to be controlled individually, except for the bow/tower hydroplanes[5].

When an external autopilot shall be tested on the submarine simulator, it should provide desired values for the mechanical angles of the hydroplanes, and perhaps the rotor RPM. Future work could include additional means to actuate the submarine simulator, this will be discussed later.

Submarine simulator The submarine simulator is the computer implementation of the submarine model. Naturally the simulation shall not be overly inefficient.

Autopilot The autopilot should include three different regions for different velocities and each region will be controlled differently. In the low velocity region, depth control shall solely be using elevator motion. In the high velocity region, depth control shall instead be performed in sledge mode, and the bow/tower hydroplanes shall be used at a minimum, or not at all. Depth changing in the region in between, shall be a combination of the two modes. The overall control performance shall be satisfying, i.e.,

- Reference tracking, no stationary errors.
- No extensive overshoots. A typical submarine performance requirement is an overshoot of maximum a few meters when changing depth.
- The measured signals shall be according to the listed sensors in section 1.1, i.e., the controller should not need internal values in the submarine simulator.

In the case of navigation system testing, references in submarine heading, depth and pitch will be given. The submarine autopilot should hence answer to references in those three.

[5] Which is often the case in real submarines

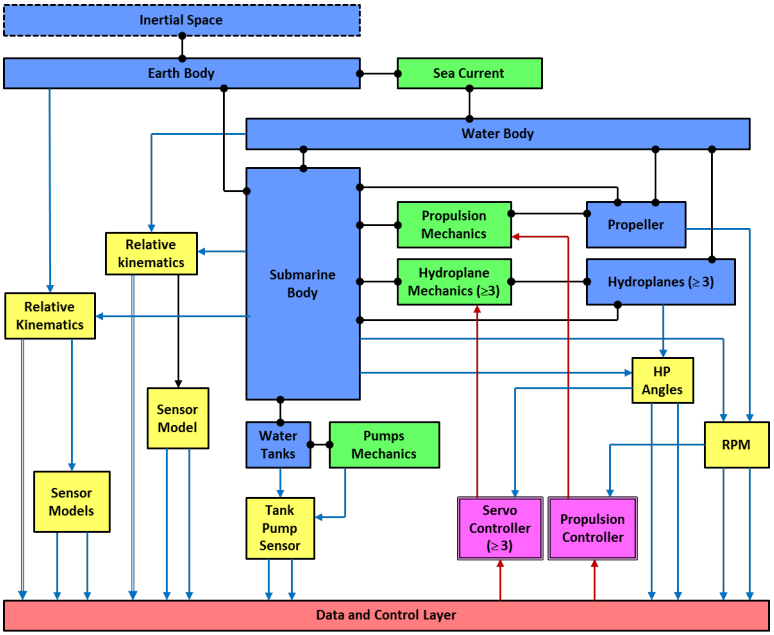

Figure 1.5: Simulator system block diagram overview.

Test rig implementation The simulator system must be compatible with an existing Saab test rig, and will therefore be implemented in C on a Linux platform. It should be able to run with the existing SASS product or another external device. To emulate the autopilot as an external device, it will be implemented separately from the submarine simulator.

Both the submarine simulator and the control system will run in real time, but asynchronous since they will run independently, and possibly on different Linux systems. The submarine simulator will be updated with 20Hz and control system with 4Hz[6]. The emphasis of this thesis should, however, be on modelling and control design.

Simulator Block diagram

Figure 1.5 shows the idea behind the simulator system as presented by Saab at the start of the thesis. This proved to be, at this stage of the simulator development, a to complex description, and had to be simplified.

[6] Which has been the case in the SASS

Delimitation

The following delimitations will be assumed:

- Completely submerged submarine.
- The submarine will be in an infinitely large ocean to avoid near surface and near bottom effects.
- No wave effects or irregular currents.
- Ideal sensors, i.e., measured value equals true value.
- Limited speed range, 4-16 knots.
- Incompressible hull.
- No tank systems (water pumping) will be modeled.

With these delimitation, Figure 1.5 could be simplified to Figure 1.6. The control part has been separated from the simulator itself, communication between them is now through the data and control layer. The sea current in Figure 1.6 is limited to constant currents that will only affect position/velocity relative earth. Also the sensor models have been removed as well as the submarine water tank actuators. The servo controllers for the hydroplanes and the propulsion will not be modeled as control loops, but rather dynamics systems with unity gain.

1.5 Individual contribution

The the physical modelling and the model implementation in Simulink was performed by Erik Lind. Magnus Meijer was responsible for porting the model into C code and, hence, the model and controller interaction in the C environment. Magnus also worked together with a consult as Saab to interface the thesis implementation with the existing program structure in the test rig. The controller was designed by Erik, but the dimensioning and weighting was performed by Magnus.

The introduction, development, and method chapters were written by Erik. Magnus wrote the theory, result, and discussion chapters.

1.6 Thesis Outline

This report consists of five Chapters, and can be summarized as follows:

Method In Chapter 2, the methods and the coordinate system notations and structures used, will be presented. This Chapter will also explain how the model was implemented in Matlab and ported to the target language C.

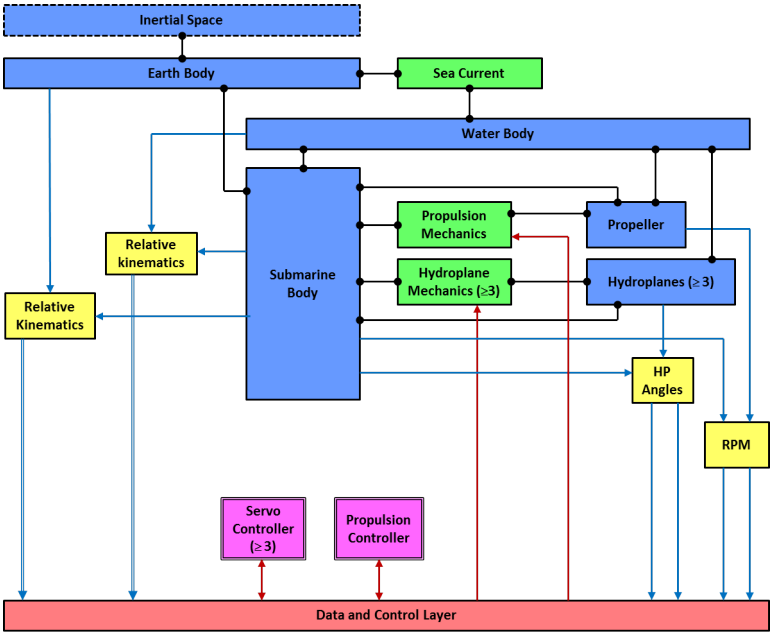

Figure 1.6: Tuned down simulator block diagram.

Theory Chapter 3 consists of theory and background of hydrodynamics and some hydrodynamic modeling. After this, equations for a six degrees of freedom dynamic body will be derived and, finally, a short collection of control designs and strategies will be presented.

Development Firstly, Chapter 4 will explain how the known hydrodynamic relations were applied to submarines, and how a model for a generic submarine model can be derived. This is followed by an introduction to a demo submarine, Finally, Chapter 4 will consist of the complete control system derivation.

Results / Simulation Chapter 5 presents the final model and autopilot, as well as plots from different simulated manoeuvres.

Discussion / Summary Chapter 6 consists of a discussion of the submarine model and control system performance. The controller itself is also analyzed, with possible oscillation and other issues. At last, ideas for future work is presented.

2

Method

2.1 Coordinate System notation

This thesis will deal with numerous different coordinate systems. In this section, the sub- and superscript notation will be shortly described.

Positions, velocities and acceleration in *(x,y,z)* are denoted **x**,**v**, and **a** respectively. For increased clarity what a vector describes and in what coordinate system it is currently expressed, sub- and superscripts will be added. Generally, vectors will be written:

$$\mathbf{x}_{BC}^{A} \tag{2.1}$$

where **x** is a vector, in this case a position vector. It could also be a velocity or acceleration vector. A is always a coordinate system abbreviation while B and C are points or coordinate systems (in such case the point will be the coordinate system origin). Equation (2.1) will thus describe the vector from point B to C expressed in the coordinate system A. For example, let A and B be two coordinate systems, $\mathbf{x}_{AB}^{B}$ is then the position of O^B relative O^A expressed in the coordinates of B. And similarly, $\mathbf{a}_{AB}^{B}$ is the acceleration of O^B relative O^A expressed in the coordinates of B, which can also be expressed as $-\mathbf{a}_{BA}^{B}$, etc.

As for angle vectors (ϕ, θ, ψ) (roll, pitch, yaw), they are defined as the rotation between two coordinate systems. Figure 2.1 describes the rotation of the *blue* frame with respect to the *black* frame. The rotations are defined in the order: yaw, pitch, and roll.

2.2 Simulator development

Matlab/ Simulink

The submarine simulator and the control system will both be implemented and tested in Matlab/Simulink due to the many advantages these software provides for this kind of task. The Simulink implementation will then be ported to C code, which is already supported. Read more about porting Simulink models to C code below.

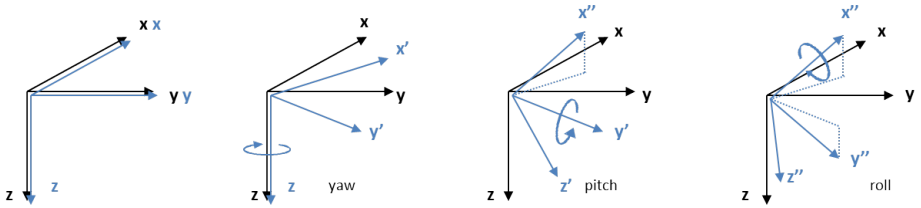

Figure 2.1: Coordinate system rotation definition, defined in the order: yaw, pitch, roll.

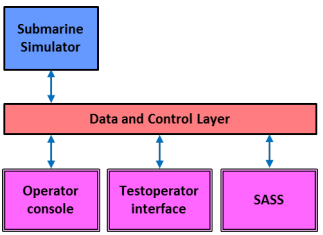

Figure 2.2: Test rig communication overview, with a SASS.

The controller and model simulator will not be updated simultaneously (20Hz vs 4Hz). Since Simulink does not support different step lengths in the same model, the dynamic parts of the controller were chosen to be implemented in discrete time to simplify the simulation in Simulink.

Communication

The idea of the final implementation structure in the test rig is illustrated in Figure 2.2. All the parts are connected through a data layer. The *test operator* will communicate with the *submarine simulator* with telnet through TCL.

If the test system is a navigation system, the test rig setup should look more like in Figure 2.3. The *SASS* has been replaced by a *navigation system*, and an *autopilot* has been connected. The *test operator* will communicate with the *submarine simulator* and *autopilot* in the same fashion as above. Communication between the *autopilot* and *submarine simulator* will be through TCP.

Code generation

Simulink features code generation for models, which produces C code that exactly represents the model simulation. If the model has inputs and outputs, they will appear as C structs in the generated code. There is also a feature to save the simulation output as a .mat file, which will be used to log data.

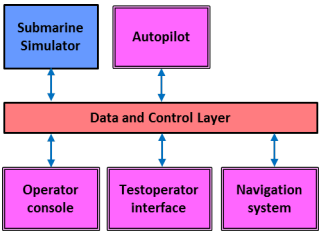

Figure 2.3: Test rig communication overview, with navigation system.

Code generation does not support variable step size simulations, but since there is a well defined update frequency, this will not be a problem. In the C code, the Simulink code generation produces a function *one_step()*, which takes the model inputs, iterates a time step, and updates the model outputs. A *main()* function is also produced by the code generation, that initializes the model and creates a for-loop that calls *one_step()* as many times as necessary for the simulation time. This is not something that will be used in this thesis, instead the *one_step()* method will be used by a scheduler that will guarantee that the model is updated with 20Hz, hence, the simulation will be in real time.

Code for the submarine simulator and the control system will be generated similarly, but with different time steps, 0.05s and 0.25s respectively. A separate scheduler for the autopilot will update the controller with 4Hz.

The two schedulers will not be synchronized, the submarine simulator and control system will operate asynchronously. But as the simulator system should correspond to a real submarine, this is actually preferred.

2.3 Schedulers

As described in Section 2.2, the simulator system will feature two schedulers for the submarine simulator and controller system. Their workflow is presented in Figure **??**. Since the submarine scheduler will update more frequently than the controller scheduler, it will call $sub_one_step()even if no TCP connection is established$.

3

Theory

3.1 Hydrodynamics

Hydrodynamics is the study of liquids in motion. A body traveling through a fluid will be exerted to a number of forces and moments, which is a result due to the physical characteristics of the liquid medium. In this section some of the different effects will be discussed and shortly explained in general, i.e., not explicitly for submarines.

Hydrostatics

Archimedes' principle states that a submerged body will experience a lifting force equal to the gravitational force of the displaced water. This force will act through the center of buoyancy [Fossen, 1994], which is the center of gravity of the displaced water, hence, this force is usually referred to as the buoyancy force. The gravity and buoyancy force will always be opposite in direction, which will cause the body to strive towards balance, i.e., when the center of buoyancy is vertically aligned with the center of gravity (Figure 3.1). The magnitudinal difference between the two forces will determine if the body will sink or float.

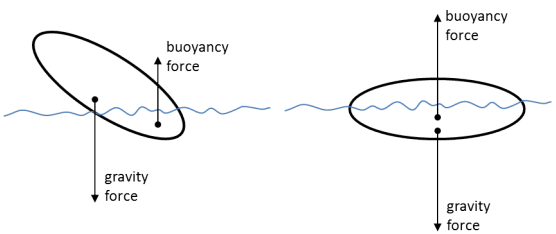

Figure 3.1: Buoyancy and gravity force.

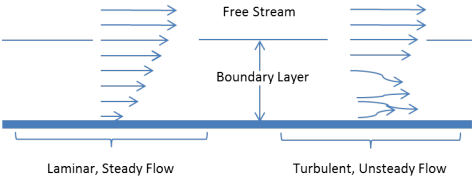

Figure 3.2: Turbulent and laminar flow.

Hydrodynamic Damping

A body traveling through a fluid will experience a drag force parallel to the incoming flow, known as hydrodynamic damping. This force is a result from numerous effects and are divided differently throughout literature and previous work. This thesis will divide the forces according to [Fossen, 1994] and [Fossen, 2011].

Pressure Drag *Pressure drag is the force normally thought of as drag. As a body travels through water, it has to suppress liquid at the front in order to move forward. This is largely dependent on the shape of the body, a more streamlined body will experience less pressure drag.*

A common way to interpret this is to view it as a pressure difference. At the front, where fluid is displaced to make room for the body, there will be an increased pressure. At the aft, the fluid will be replaced into the space the body left behind, the pressure instead will be lower. This pressure difference will induce a force, similar to a airplane wing or sail lifting forces. A less streamlined aft will also create turbulence which will further decrease the pressure at the aft and thus further increase the drag force.

Friction Drag *Friction drag arises from friction between the body and the surrounding fluid. When a body travels through water, it will accelerate the fluid closest to its surface. This flow can be seen as parallel layers of fluid with friction in between. This will cause the different layers to have different velocities, decreasing with the distance from the body, as seen in Figure 3.2.*

The flow may be laminar or turbulent, or a combination of the both. Laminar flow is when there is no disruption between the parallel layers flowing past the body. This occurs at low velocities and gives rise to very low friction and noise. As the velocity increases the different layers of fluid overturns and causes turbulence, see Figure 3.2. This is very energy consuming, and causes high friction and noise.

Wave Damping *Wave damping is the resistance experienced by the body when advancing through waves on the surface. This effect is the most important damping contributor in rough seas, due to the fact that the forces from the waves are proportional to the square of the wave height [Fossen, 2011]. This effect is neglected in this thesis due to the delimitation presented in Section 1.4, i.e., the body will be*

completely submerged at a great depth, and therefore not affected by surface waves.

Potential Damping *Potential damping refers to the energy loss when a body is forced to oscillate up and down with the surface waves. Due to the same reasons as for wave damping, this effects is not taken into account in this thesis.*

Drag coefficient

The effects of drag, at a certain velocity, is usually described by a non-dimensional drag coefficient, defined as:

$$C_d = \frac{-F}{\frac{1}{2} \cdot \rho \cdot A \cdot u^2} \tag{3.1}$$

where F is the drag force, ρ is the density of the fluid, A is the area shown to the flow and u the velocity of the body. For certain applications it is more common to normalize with the area of the submerged hull, referred to as the wetted surface. In a velocity interval, the drag coefficient is only marginally changing and Equation (3.1) *can instead be used to calculate the resistance for a given velocity:*

$$F = -C_d \cdot \frac{1}{2} \cdot \rho \cdot A \cdot u^2 \tag{3.2}$$

Reynolds number *Reynolds number is the relation between the inertial- and the viscous forces of a fluid. It is defined in open sea situations as [Fossen, 2011]:*

$$R_n = \frac{uD}{\nu} \tag{3.3}$$

where D is the characteristic length of body, u is the velocity and ν is the kinematic viscosity coefficient of the fluid. A high Reynold's number means the flow is mainly turbulent, while a lower generally corresponds to a more laminar flow.

Lift *When an object is traveling through a medium, it will experience lift forces perpendicular to the incoming flow. This effect is caused by pressure changes between the top and bottom surfaces. The classical example is an airfoil traveling through air, see Figure 3.3. When the air is deflected it will have to travel around the airfoil. Since the air above the wing will have to travel further than the air below, the pressure will decrease on the top surface, and create a lift force on the airfoil.*

The lift generated is highly dependent on the angle of attack, i.e. the angle of the velocity vector of the incoming flow. A perfectly symmetrical airfoil will produce no lift if the angle of attack is zero, but if it is tilted, there will be a pressure difference and a lift force is generated.

All bodies moving through a medium will experience this effect. The hydroplanes can be compared with airfoils and will produce a great amount of lift when actuated. When manoeuvring the submarine, the incoming flow will change, and thus the submarine tower and hull will also generate lift forces.

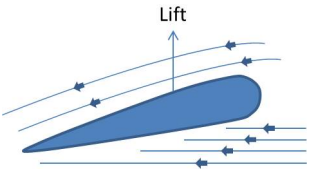

Figure 3.3: Flow past an airfoil.

Added mass *When a body travels through water, the hull friction will accelerate the water closest to the hull, creating a layer of moving water. The closest layer will in turn accelerate the next layer of water and so on. Hence, there will be an region of moving water around the body.*

When the body accelerates, it will also have to accelerate the water closest to the hull. When it turns, it will have to turn the water that is traveling with the body. This effect is called the added mass effect since the body will appear heavier than it is. This will effect both the apparent mass and inertia of the body.

The added mass effect does also affect bodies moving through the air, but since the mass of the accelerated air is often negligible compared to the body mass, this is rarely accounted for. The accelerated water, however, does have a considerable mass and will have to be taken into account when modelling bodies in water.

It is difficult to calculate how large this effect will be, since it heavily depends on the shape and roughness of the submarine, it is therefore usually analyzed with experiments.

Control Surfaces

To be able to control the attitude of a submarine, several control surfaces are used as described in Section 1.1.

Hydrodynamic Forces *A hydroplane will both experience a drag force opposite to the direction of the incoming flow, and a lift force perpendicular to it. [Toxopeus, 2011] proposes a way to calculate the drag and lift forces, D_{ru} and L_{ru}, see Figure 3.4,*

$$L_{ru} = \frac{1}{2} \cdot \rho \cdot V_r^2 \cdot A_R \cdot C_l \cdot \cos \delta_e \cdot \sin \delta_e \tag{3.4}$$

$$D_{ru} = \frac{1}{2} \cdot \rho \cdot V_r^2 \cdot A_R \cdot C_d \cdot \sin^2 \delta_e \tag{3.5}$$

where V_r is the velocity of the inflowing water, A_R is the area of the rudder, C_l is the lift coefficient, δ_e is the so called effective rudder angle, and C_d is the drag coefficient. [Toxopeus, 2011] defines two angles, the hydrodynamic rudder angle, δ_h and the effective rudder angle δ_e. δ_h is the angle between the ship longitudinal axis and the incoming flow, the effective rudder angle δ_e is the angle between the mechanical rudder angle δ and δ_h, see Equation (3.6)*. As the name suggests, δ_e is*

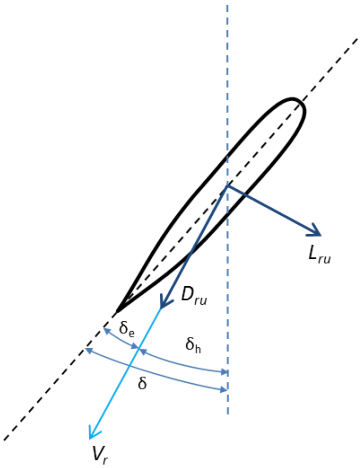

Figure 3.4: Rudder forces according to [Toxopeus, 2011]. Note that D_{ru} is opposite the direction of the incoming flow, and that L_{ru} is perpendicular to it

the rudder angle for which a force is generated, i.e., when δ_e is zero, no force is created.

$$\delta_e = \delta - \delta_h \tag{3.6}$$

In equation (3.6), $\delta_h = \arctan(\frac{v_y}{v_x})$ *where v_y and v_x are the x and y components of the water velocity at the rudder. This translates to the body longitudinal and lateral forces and yaw moment:*

$$F_x = -D_{ru} \cdot \cos\delta_h - L_{ru} \cdot \sin\delta_h \tag{3.7}$$

$$F_y = L_{ru} \cdot \cos\delta_h - D_{ru} \cdot \sin\delta_h \tag{3.8}$$

$$\tau = \boldsymbol{x} \times (F_x, F_y, 0) \tag{3.9}$$

where $\boldsymbol{x}$ is the position of the rudder. The rudder drag and lift coefficients are usually experimentally determined, but [Toxopeus, 2011] refers to previously derived empiric formulas for calculating them.

$$C_l = \frac{6.13 \cdot \Lambda}{2.25 + \Lambda} \tag{3.10}$$

$$C_d = \frac{C_l^2}{\pi \cdot \Lambda} \tag{3.11}$$

where C_l is the lift coefficient, C_d the drag coefficient, and Λ the so called rudder aspect ratio, $\Lambda = \frac{length}{area}$.

Flow Straightening *When a submarine is moving, the water flow vortex along the hull will alter the water flow at the rudders. [Toxopeus, 2011] suggests a method to compensate for this phenomena by adding a flow straightening coefficient for the hydrodynamic rudder angle δ_h, i.e., decreasing it. This will be neglected in this thesis.*

Flow straightening is enhanced by the propeller, greatly so when it is placed in front of the rudders. Although, for modern submarines, propellers are most often placed behind the hydroplanes, in order to decrease noisy turbulence around the rudders.

Propulsion

The propeller converts rotational motion into forward/backward thrust. To calculate the thrust F_p and torque τ_p, [Toxopeus, 2011] and [Watt, 2007] among others, suggests calculating dimensionless thrust and torque coefficients which only depend on the advance ratio J:

$$K_t(J) = \frac{F_p}{\rho n^2 D_p^4} \tag{3.12}$$

$$K_q(J) = \frac{\tau_p}{\rho n^2 D_p^5} \tag{3.13}$$

$$J = \frac{v_p}{nD_p} \tag{3.14}$$

where F_p is the force exerted by the propeller, τ_p is the torque generated, n is the RPS[1]*, D_p is the diameter of the propeller, and v_p is the velocity of the incoming flow. The functions $K_t(J)$ and $K_q(J)$ are determined by water tests or advanced computer calculations, when the propeller is operating at different advance ratios. Equation* (3.12) *and* (3.13) *can then be used for determining the thrust and torque.*

$$F_p = K_t \cdot \rho n^2 D_p^4 \tag{3.15}$$

$$\tau_p = K_q \cdot \rho n^2 D_p^5 \tag{3.16}$$

The propeller on a submarine is operating in a wake from the hull which reduces the average inflow to the propeller. This is usually corrected with a one-dimensional correction factor w_T: [Toxopeus, 2011]:

$$v_p = (1 - w_T) \cdot u \tag{3.17}$$

where w_T if the so called Taylor wake fraction, and u the forward velocity of the submarine. Since the propeller accelerates water backwards, it generates a negative pressure on the hull upstream from its position. This will increase the drag force

[1] Revolutions Per Second

on the hull, negating some of the propeller thrust. This can be corrected with another constant, also suggested by [Toxopeus, 2011], known as the thrust deduction fraction t:

$$F_{res} = (1-t) \cdot F_p \tag{3.18}$$

To determine w_T and t, model experiments must be performed on the hull alone to determine the wake fraction, as well as the hull with the propeller attached to determine the thrust deduction factor.

Cavitation *Cavitation is caused when forces acting on a liquid forms small cavities or bubbles. This is usually a result of rapid pressure changes, for example around a propeller. If the small cavities implode, they will generate an intense shockwave. This is an undesired behaviour since repeated implosions are noisy and causes heavy wear on materials.*

3.2 6 degrees of freedom dynamics

A rigid body's movement and position in a three dimensional space can uniquely be described using six states. Its position can be determined with Cartesian (x,y,z) coordinates, and its turn by three angles (ϕ,θ,ψ) (which are the rotations around the x-,y- and z- axes respectively). These six coordinates result in a system with six degrees of freedom. In this section the dynamics of such a system will be derived.

Consider a space-fixed coordinate system W and a body-fixed frame REF with the origins O^W and O^R respectively. Let $\boldsymbol{a}_G$ be the acceleration and $\boldsymbol{x}_G$ the position of the the center of mass. Let $\boldsymbol{v}$ be the velocity and $\boldsymbol{\omega}$ the angular velocity of O_R expressed in the body-fixed coordinates REF. The acceleration $\boldsymbol{a}_G$ is given by the Newton-Euler equations from classic mechanics: [Fossen and Fjellstad, 1995]

$$\boldsymbol{a}_G = \frac{\partial \boldsymbol{v}}{\partial t} + \boldsymbol{\omega} \times \boldsymbol{v} + \dot{\boldsymbol{\omega}} \times \boldsymbol{x}_G + \boldsymbol{\omega} \times (\boldsymbol{\omega} \times \boldsymbol{x}_G) \tag{3.19}$$

In order to simplify the readability of Equation (3.19) *the standard vector notation was circumvented and will instead be presented in Table 3.1.*

With forces $(F_x,F_y,F_z)_i$ acting on the origin O^R, the movement of the body will be:

$$\sum (F_x,F_y,F_z)_i = m\boldsymbol{a}_G \tag{3.20}$$

where m is the mass.

Angular momentums τ_i around O^R results in the movements:

$$\sum \tau_i = \boldsymbol{J}\dot{\boldsymbol{\omega}} + \boldsymbol{\omega} \times \boldsymbol{J}\boldsymbol{\omega} + \boldsymbol{x}_G \times \boldsymbol{a}_G \tag{3.21}$$

where $\boldsymbol{J}$ is the moment of inertia matrix. Equations (3.19) *and* (3.21) *will be combined, i.e., substitute $\boldsymbol{a}_G$ from* (3.19) *in* (3.21)*, to create the angular acceleration.*

$\mathbf{x}_G$	$\mathbf{x}_{RG}^R$
$\mathbf{a}_G$	$\mathbf{a}_{RG}^R$
$\mathbf{v}$	$\mathbf{v}_{WR}^R$
ω	ω_{WR}^R

Table 3.1: The vectors in Section 3.2 written with the standard notation

3.3 Control designs

In this Section a very short summary of a few different control designs used in this thesis are discussed. For more information, see [Glad and Ljung, 2003].

PID

The PID-controller is the most common type of feedback controller throughout industry. It consists of three parts, the proportional part P, the integral part I, and the derivative part D. The controller tries to minimize the control error, that is, the difference between a desired setpoint and the measured output of the process. The PID-controller output $u(t)$ is defined as[2].

$$u(t) = K_p \cdot e(t) + K_i \cdot \int_0^t e(\tau)d\tau + K_d \cdot \frac{d}{dt}e(t) \tag{3.22}$$

where K_p, K_i and K_d are the tunable gain parameters for the proportional, integral respective the derivative parts and $e(t) = r(t) - y(t)$, is the control error.

PID Tracking *Switching between multiple PIDs in a controller system is not uncommon. The different controllers are most certainly dimensioned differently, hence, the control signal will suffer a step at the time of the switch. In order to avoid behaviour like this, it is possible to implement PID tracking, where the non active controllers follow the output of the active one. PID tracking is implemented in Simulink as in Figure 3.5*

State Feedback

A system on standard state space form is written as in Equation 3.23.

$$\begin{aligned} \dot{\boldsymbol{x}} &= \boldsymbol{A}\boldsymbol{x} + \boldsymbol{B}\boldsymbol{u} \\ \boldsymbol{y} &= \boldsymbol{C}\boldsymbol{x} + \boldsymbol{D}\boldsymbol{u} \end{aligned} \tag{3.23}$$

When controlling a system on state space form, a popular control method is the so called state feedback control, where the control signal $\boldsymbol{u}$ is the state vector $\boldsymbol{x}$ multiplied by a feedback gain matrix $\boldsymbol{L}$. This allows the control engineer to place

[2] This is the most basic of PID controller definitions, other variants do exist

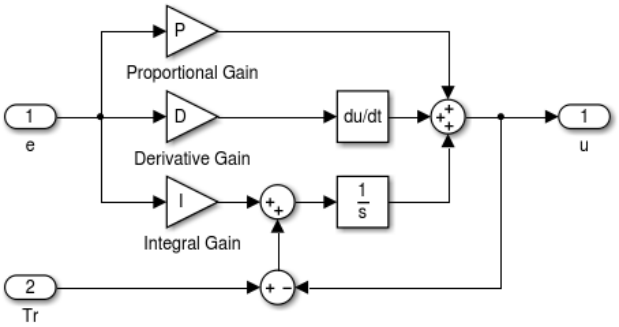

Figure 3.5: PID tracking implementation.

the closed loop poles freely in the s-plane[3]*. This is desirable since the poles greatly influence the response of a system.*

The poles of an open loop system are given by the roots of characteristic equation $|s\boldsymbol{I}-\boldsymbol{A}|=0$*. With state feedback, the control signal* $\boldsymbol{u}$ *takes the form* $\boldsymbol{u}=-\boldsymbol{L}\boldsymbol{x}$*, the system in Equation* (3.23) *can then be written as:*

$$\begin{aligned}\dot{\boldsymbol{x}} &= (\boldsymbol{A}-\boldsymbol{B}\boldsymbol{L})\boldsymbol{x}\\ \boldsymbol{y} &= (\boldsymbol{C}-\boldsymbol{D}\boldsymbol{L})\boldsymbol{x}\end{aligned} \tag{3.24}$$

The new characteristic equation

$$\det(s\boldsymbol{I}-(\boldsymbol{A}-\boldsymbol{B}\boldsymbol{L})) \tag{3.25}$$

The new characteristic equation takes the form in Equation (3.24)*, where* $\boldsymbol{L}$ *is chosen to place the poles at the desired locations.*

Observer

When using state feedback controllers for system control, all the states have to be known. This is often not the case, since rarely all are measured. Some states might not even have a direct physical interpretation, which complicates measuring further. A state feedback controller therefore has to be complemented with an observer. An observer estimates the unknown states[4] *from the input to the system and the known (measured) output signals, and feeds them to the controller (Equation* (3.26)*).*

$$\begin{aligned}\dot{\hat{\boldsymbol{x}}} &= \boldsymbol{A}\hat{\boldsymbol{x}}+\boldsymbol{B}\boldsymbol{u}+\boldsymbol{K}(\boldsymbol{y}-\boldsymbol{C}\hat{\boldsymbol{x}})\\ \boldsymbol{u} &= -\boldsymbol{L}\hat{\boldsymbol{x}}\end{aligned} \tag{3.26}$$

[3] If the system is controllable.
[4] This is possible if the system is observable.

where $\hat{\boldsymbol{x}}$ is the observed state vector and $\boldsymbol{K}$ the observer gain matrix, which will be dimensioned to create the desired observer dynamics. A common way of doing this is by letting the observer gain matrix be a Kalman filter, which is an optimal observer with respect to measurement noise and process disturbances[5]*. As the name suggests, the Kalman filter is not only an observer, but a filter, that prevents measurement noise to be fed back into the system.*

Optimal control - LQG

A method of dimensioning the state feedback control of a system, is by using Linear Quadratic Gaussian control theory. The idea of LQG is to minimize a quadratic cost function, which will yield an optimized controller with respect to certain weights on the controlled variables and control efforts:

$$min(||\boldsymbol{e}||_{\boldsymbol{Q}}^2 + ||\boldsymbol{u}||_{\boldsymbol{R}}^2) = min \int \boldsymbol{e}^T(t)\boldsymbol{Q}\boldsymbol{e}(t) + \boldsymbol{u}^T(t)\boldsymbol{R}\boldsymbol{u}(t)dt \tag{3.27}$$

where $\boldsymbol{Q}$ and $\boldsymbol{R}$ are the weight matrices for the error $\boldsymbol{e}(t)$ and control signal $\boldsymbol{u}(t)$. These are used to weigh the control effort against the control error, i.e., how to penalize the different control errors, and the different control signals.

To determine the optimal controller, the system is written on the general state space form used in [Glad and Ljung, 2003]:

$$\begin{aligned} \dot{\boldsymbol{x}} &= \boldsymbol{A}\boldsymbol{x} + \boldsymbol{B}\boldsymbol{u} + \boldsymbol{N}\boldsymbol{v}_1 \\ \boldsymbol{z} &= \boldsymbol{M}\boldsymbol{x} \\ \boldsymbol{y} &= \boldsymbol{C}\boldsymbol{u} + \boldsymbol{v}_2 \end{aligned} \tag{3.28}$$

where $\boldsymbol{v}_1$ is a white Gaussian disturbance vector and $\boldsymbol{z}$ are the controlled variables. $\boldsymbol{v}_2$ is the measurement noise, also of white Gaussian characteristic. Consider the system above, where $\left[\begin{smallmatrix} v_1 \\ v_2 \end{smallmatrix}\right]$ are stochastic noise with intensity $\left[\begin{smallmatrix} R_1 & R_{12} \\ R_{12}^T & R_2 \end{smallmatrix}\right]$. The sought feedback, $\boldsymbol{u}_{FB} = -\boldsymbol{L}\hat{\boldsymbol{x}}$ will minimize the expression [Glad and Ljung, 2003]:

$$||z||_Q^2 + ||u||_R^2 \tag{3.29}$$

The feedforward control part $\boldsymbol{u}_{FF} = \boldsymbol{L}_r\boldsymbol{r}$ will be dimensioned to ensure that the closed loop gain is identity:

$$\boldsymbol{M}(\boldsymbol{B}\boldsymbol{L} - \boldsymbol{A})\boldsymbol{B} \cdot \boldsymbol{L}_r = \boldsymbol{I} \tag{3.30}$$

The observer gain matrix $\boldsymbol{K}$ will create the perfect trade off between the system model and the measured output.

[5] The Kalman filter assumes white Gaussian noise and disturbances.

4

Development

4.1 Modelling of a submarine

The dynamics of a body with six degrees of freedom where presented in Section 3.2. This Section will apply those equations to a submarine submerged in water and try to model the external forces $\boldsymbol{F}_i = (F_x, F_y, F_y, \tau_x, \tau_y, \tau_z)_i$ which are hydro-static and hydro-dynamic forces and torques, as well as propulsion and hydroplane forces and moments.

Coordinate Systems and notation

The following coordinate systems will be extensively used:

Name	*abbr.*[1]	*subs.*[2]	*explanation*	*x,y,z corresponds to*
Lon/lat	*LL*	*L*	*Earth fixed*	*longitude, latitude, depth*
Water	*W*	*W*	*Water fixed*	*north, east, down*
Reference	*REF*	*R*	*Body fixed in the center of buoyancy*	*bow, starboard, down*
Center of gravity	*G*	*G*	-	*bow, starboard, down* $x^R_{RG} = (x_G, y_G, z_G)$

Earth frame *A position in LL is given by (longitude, latitude, depth), which will be denoted by $(x, y, z)^L$.*

Water frame *The $(x, y, z)^W$ axes corresponds to (north, east, down)-directions. The origin of W moves with the water currents which means that the relation between W and LL is a simple translation in the $(x, y)^L$- plane that varies with time.*

[1] abbreviation
[2] subscripts

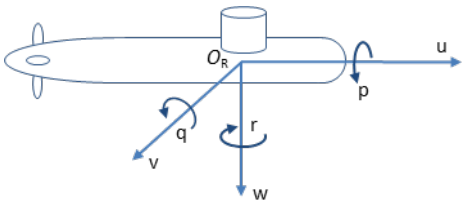

Figure 4.1: Reference frame velocity notation.

Reference frame *The REF frame is submarine-fixed and the origin is placed in the center of buoyancy. This is preferable since the center of buoyancy rarely changes while the center of gravity depend on load and the condition of the different tanks. As for the REF coordinate system, the axes will be denoted* $(x,y,z)^R$ *and the velocities according to the standard convention used in literature*[3] (u,v,w)*, i.e.* $(\dot{x},\dot{y},\dot{z})^R_{WR}$*, and* (p,q,r) *for the angular velocities, see Figure 4.1. For the forces and moments,* $\boldsymbol{F} = (F_x,F_y,F_y,\tau_x,\tau_y,\tau_z)^R_{WR} = (X,Y,Z,K,M,N)$ *will be used, as is also the standard.*

The relation between (p,q,r) *and* $(\dot{\phi},\dot{\theta},\dot{\psi})$ *are:*

$$\begin{aligned}\dot{\phi} &= p + q\sin\phi\tan\theta + r\cos\phi\tan\theta \\ \dot{\theta} &= q\cos\phi - r\sin\phi \\ \dot{\psi} &= q\frac{\sin\phi}{\cos\theta} + r\frac{\cos\phi}{\cos\theta}\end{aligned} \tag{4.1}$$

Submarine six degrees of freedom

The W and REF frames in Section 3.2 will indeed be the water and body frames. With this notation, Equation (3.20) *and* (3.21) *correspond to:*

$$m(\dot{u} - vr + wq - x_G(q^2+r^2) + y_G(pq - \dot{r}) + z_G(pr + \dot{q})) = \sum X_i \tag{4.2a}$$

$$m(\dot{v} - wp + ur - y_G(r^2+p^2) + z_G(qr - \dot{p}) + x_G(qp + \dot{r})) = \sum Y_i \tag{4.2b}$$

$$m(\dot{w} - uq + vp - z_G(p^2+q^2) + x_G(rp - \dot{q}) + y_G(rq + \dot{p})) = \sum Z_i \tag{4.2c}$$

$$I_x\dot{p} + (I_z - I_y)qr - (\dot{r} + pq)I_{zx} + (r^2 - q^2)I_{yz} + (pr - \dot{q})I_{xy} = \sum K_i \tag{4.2d}$$

$$I_y\dot{q} + (I_x - I_z)rp - (\dot{p} + qr)I_{xy} + (p^2 - r^2)I_{zx} + (qp - \dot{r})I_{yz} = \sum M_i \tag{4.2e}$$

$$I_z\dot{r} + (I_y - I_x)pq - (\dot{q} + rp)I_{yz} + (q^2 - p^2)I_{xy} + (rq - \dot{p})I_{zx} = \sum N_i \tag{4.2f}$$

[3] defined by SNAME (1950)

The Equations (4.2) *are nonlinear and quite complex, neither do they explicitly state expressions for* $(\dot{u},\dot{v},\dot{w},\dot{p},\dot{q},\dot{r})$. *However, Equations* (4.2) *are linear in sense of* $(\dot{u},\dot{v},\dot{w},\dot{p},\dot{q},\dot{r})$ *and can thus be solved by a matrix inversion. Modeling a submarine is now divided into modeling the different forces and moments in the 6 directions.*

External Forces

The effects and forces from Section 3.1 are summarized as:

$$\sum \boldsymbol{F}_i = \boldsymbol{F}_{HS} + \boldsymbol{F}_{HD} + \boldsymbol{F}_P + \boldsymbol{F}_C \tag{4.3}$$

where $\boldsymbol{F}_{HS}$ *are the hydrostatic forces and moments, i.e., gravity and buoyancy forces,* $\boldsymbol{F}_{HD}$ *are the hydrodynamic forces from added mass and inertia, drag and cross flow,* $\boldsymbol{F}_P$ *are the propulsion forces, and* $\boldsymbol{F}_C$ *are forces from the control surfaces, i.e., the different hydroplanes. The forces and moments are now collected in the Equations* (4.4).

$$\sum X_i = X_{HS} + X_{HD} + X_P + X_C \tag{4.4a}$$
$$\sum Y_i = Y_{HS} + Y_{HD} + Y_C \tag{4.4b}$$
$$\sum Z_i = Z_{HS} + Z_{HD} + Z_C \tag{4.4c}$$
$$\sum K_i = K_{HS} + K_{HD} + K_P + K_C \tag{4.4d}$$
$$\sum M_i = M_{HS} + M_{HD} + M_C \tag{4.4e}$$
$$\sum N_i = N_{HS} + N_{HD} + N_C \tag{4.4f}$$

This is a common way of interpreting and dividing forces acting on a submarine in papers and literature. The extra terms in the x^R*- direction and rotation about the* x^R*- axis are due to the propulsion and induced torque from the propeller. This assumes that, that the rotor is perfectly aligned with the center of buoyancy* $\boldsymbol{x}^R_{RB}$ *in the* $(y,z)^R$*- plane which is rarely true. More accurate would be to also introduce a pitch moment due to rotor propulsion, however, this lever arm would probably be small and therefore, this effect is therefore not accounted for.*

Hydrostatic forces

For a 6 DOF body, the hydrostatic forces in Section 3.1 are calculated as: [Feldman, 1979].

$$\begin{pmatrix} X_{HS} \\ Y_{HS} \\ Z_{HS} \\ K_{HS} \\ M_{HS} \\ N_{HS} \end{pmatrix} = \begin{pmatrix} -(W-B)\sin\theta \\ (W-B)\cos\theta\sin\phi \\ (W-B)\cos\theta\cos\phi \\ (y_G W - y_B)\cos\theta\cos\phi - (z_G W - z_B B)\cos\theta\sin\phi \\ -(x_G W - x_B B)\cos\theta\cos\phi - (z_G W - z_B B)\sin\theta \\ (x_G W - x_B B)\cos\theta\sin\phi - (y_G W - y_B B)\sin\theta \end{pmatrix} \tag{4.5}$$

where W *is the gravity force and* B *is the buoyancy force.*

Hydrodynamic derivatives

Hydrodynamics is a very complex phenomena and physically very hard to model. Most of the formulas derived are empirical and they should thus be used with certain care. Many authors deal with the subject of hydrodynamics by replacing $\boldsymbol{F}_{HD}$ *with a coefficient based model, with terms like* $X_{u|u|}u|u|$*, cross terms like* $X_{uy}uy$ *and derivative terms like* $X_{\dot{u}}\dot{u}$ *or* $X_{\dot{q}}\dot{q}$*. For example. the forces in* x^R*- direction could look something like this: [Ridley et al., 2003]*

$$\begin{aligned}\sum X_i =& X_{HS} + X_P + X_C + X_{u|u|}u|u| + X_{\dot{u}}\dot{u} + X_{uv}uv + X_{vw}vw + X_{v|v|}v|v| + \\ & X_{vr}vr + X_{w|w|}v|w| + X_{wq}wq + X_{qq}qq + X_{rr}rr\end{aligned} \tag{4.6}$$

The equations for $(X,Y,Z,K,M,N)_i$ *differ slightly throughout previous works.* $X_{u|u|}$ *and* $X_{v|v|}$ *describes how movement in X- and Y- direction creates a longitudinal force, which will be relative to the signs of u and v.* $X_{\dot{u}}$ *is the induced force in* x^R*- direction due to acceleration.* X_{uv} *describes a force along* x^R *due to combined u and v movement. Similarly,* X_{vw} *models how a combined movement in v and w creates a force in* x^R*- direction etc. The terms including an absolute value of a velocity is interpreted as a drag term, since they are quadratic and relative to the direction. The derivative subscript terms, e.g.,* $X_{\dot{u}}$*, try to model the apparent increased mass due to water acceleration around the hull, as described in Section 3.1. The cross terms, e.g.,* X_{uv}*, are forces from combined movements in different directions which arise due to the accelerated water around the hull. The sum of the different terms can be seen as a Taylor expansion and the coefficients are often called hydrodynamic derivatives, i.e.:*

$$X_{\dot{u}} = \frac{\partial X}{\partial \dot{u}} \tag{4.7}$$

Because of this, one could of course model a submarine with a Taylor expansion of higher order. However, this is unusual in previous works in this subject in order to avoid unwanted behaviour to far from the operating point, i.e., outside some interval of validity. The reader will probably notice that the Taylor expansion in Equation (4.6) *does not include all the possible combinations of* (u,v,w,p,q,r)*, this is because some are considered zero, or at least small, which will be shown.*

The added mass terms add additional $\dot{u},\dot{v},\ldots,\dot{r}$ *terms to Equation* (4.2)*, which are collected into the symmetric added mass matrix [Fossen, 2011]:*

$$F_{HD} = \begin{pmatrix} X_{\dot{u}} & X_{\dot{v}} & X_{\dot{w}} & X_{\dot{p}} & X_{\dot{q}} & X_{\dot{r}} \\ Y_{\dot{u}} & Y_{\dot{v}} & Y_{\dot{w}} & Y_{\dot{p}} & Y_{\dot{q}} & Y_{\dot{r}} \\ Z_{\dot{u}} & Z_{\dot{v}} & Z_{\dot{w}} & Z_{\dot{p}} & Z_{\dot{q}} & Z_{\dot{r}} \\ K_{\dot{u}} & K_{\dot{v}} & K_{\dot{w}} & K_{\dot{p}} & K_{\dot{q}} & K_{\dot{r}} \\ M_{\dot{u}} & M_{\dot{v}} & M_{\dot{w}} & M_{\dot{p}} & M_{\dot{q}} & M_{\dot{r}} \\ N_{\dot{u}} & N_{\dot{v}} & N_{\dot{w}} & N_{\dot{p}} & N_{\dot{q}} & N_{\dot{r}} \end{pmatrix} \begin{pmatrix} \dot{u} \\ \dot{v} \\ \dot{w} \\ \dot{p} \\ \dot{q} \\ \dot{r} \end{pmatrix} + \ldots \tag{4.8}$$

Rearranging Equation (4.2) *with only derivative terms on the left hand side yields:*

$$\begin{pmatrix} m & 0 & 0 & 0 & mz_G & -my_G \\ 0 & m & 0 & -mz_G & 0 & mx_G \\ 0 & 0 & m & my_G & -mx_G & 0 \\ 0 & -mz_G & my_G & I_x & -I_{xy} & -I_{zx} \\ mz_G & 0 & -mx_G & -I_{xy} & I_y & -I_{yz} \\ -my_G & mx_G & 0 & -I_{zx} & -I_{yz} & I_z \end{pmatrix} \begin{pmatrix} \dot{u} \\ \dot{v} \\ \dot{w} \\ \dot{p} \\ \dot{q} \\ \dot{r} \end{pmatrix} = \dots \tag{4.9}$$

Moving the added mass term in Equation (4.8) *to the left hand side and combining with Equation* (4.9) *gives:*

$$\begin{pmatrix} m-X_{\dot{u}} & -X_{\dot{v}} & -X_{\dot{w}} & -X_{\dot{p}} & mz_G-X_{\dot{q}} & -my_G-X_{\dot{r}} \\ -Y_{\dot{u}} & m-Y_{\dot{v}} & -Y_{\dot{w}} & -mz_G-Y_{\dot{p}} & -Y_{\dot{q}} & mx_G-Y_{\dot{r}} \\ -Z_{\dot{u}} & -Z_{\dot{v}} & m-Z_{\dot{w}} & my_G-Z_{\dot{p}} & -mx_G-Z_{\dot{q}} & -Z_{\dot{r}} \\ -K_{\dot{u}} & -mz_G-K_{\dot{v}} & my_G-K_{\dot{w}} & I_x-K_{\dot{p}} & -I_{xy}-K_{\dot{q}} & -I_{zx}-K_{\dot{r}} \\ mz_G-M_{\dot{u}} & -M_{\dot{v}} & -mx_G-M_{\dot{w}} & -I_{xy}-M_{\dot{p}} & I_y-M_{\dot{q}} & -I_{yz}-M_{\dot{r}} \\ -my_G-N_{\dot{u}} & mx_G-N_{\dot{v}} & -N_{\dot{w}} & -I_{zx}-N_{\dot{p}} & -I_{yz}-N_{\dot{q}} & I_z-N_{\dot{r}} \end{pmatrix} \tag{4.10}$$

which is the so called mass matrix, which will be denoted ***M****. Since the submarine accelerates water around its hull, the apparent mass will increase which means that at least the diagonal elements of Equation* (4.8) *should be negative, in order to increase the diagonal elements in Equation* (4.10)*.*

Due to hull symmetry, many of these added mass coefficients are zero. For submarines, it is common to assume symmetry about the xz- plane which leads to the following terms being zero, some of these due to symmetry in the added mass matrix [Watt, 2007]

$$X_{\dot{v}}, X_{\dot{p}}, X_{\dot{r}}, Y_{\dot{u}}, Y_{\dot{w}}, Y_{\dot{q}}, Z_{\dot{w}}, Z_{\dot{p}}, Z_{\dot{q}}, K_{\dot{u}}, K_{\dot{w}}, K_{\dot{q}}, M_{\dot{v}}, M_{\dot{q}}, M_{\dot{r}}, N_{\dot{u}}, N_{\dot{w}}, N_{\dot{q}} = 0 \tag{4.11}$$

Determine hydrodynamic coefficients

Model testing *A common method of determining hydrodynamics coefficients is to experiment on a small replica of the vessel in a laboratory pool. This method can be considered to be the most accurate since there are no assumptions or simplifications involved. The coefficients derived for the model will then be scaled to fit a full scale. These coefficients may be accurate for the model, but some accuracy is lost due to nonlinearity in the equations, and non scaling water viscosity [Larsson and Raven, 2010]. During the testing, the model is forced into certain manoeuvres and the forces on the hull are measured [Åström and Källström, 1976].*

Real testing *Another alternative is to derive the coefficient through actual full scale testing, as previously done in [Åström and Källström, 1976], where the coefficients for a freighter and a tanker where derived through actual testing. An issue with this is the cost, especially for submarines where the operating costs are huge.*

As also pointed out by [Åström and Källström, 1976], for a full identification to be possible, information about the motion in all the possible degrees of freedom is necessary. For a surface going vessel this means you need to measure, u, v, and r, and for a submarine with 6 DOF you need to measure all the six movements $u, v, r, p, w,$ and r for a proper system identification.

Computational fluid dynamics (CFD) *Computational fluid dynamics, is the generic name for software used to simulate fluid motion and force on submerged or partly submerged bodies. They have not yet been fully accepted in the scientific community and pool testing is still preferred when designing hulls. However, with increased computational capacity in the every day computer, CFD softwares are becoming more and more popular in prediction of ship motion. This can be seen by the numerous reports in the last years where authors simulate ship motion or derive the hydrodynamic coefficients through a CFD software, .e.g., [Toxopeus, 2011].*

Prediction formulas *Despite the lack of manageable analytic theory in the subject of hydrodynamics, there do exist some partly analytic, partly empirical, formulas in predicting added mass terms for submarines.*

Ship manoeuvring forces

One of the difficulties with hydrodynamic modelling, is to model hydrodynamic forces when turning, i.e., drifting. Hydrodynamics coefficients in steady state are somewhat constant but when the state change, the water flow around the hull changes direction and with that the hydrodynamic derivatives. As for the hull drag, a simple way of tackle this is to divide the flow into components and let the drag force in the different directions act on the water's relative inflow speed. That is, the drag force in y^R is a function of the sway v and the yaw r, and correspondingly, the force in the x^R- direction is a function of the surge u. The problem with this method is that the inflowing water sees a different shape and effective area in case of a drift, which means that the drag coefficients do in a way change with the angle of drift. A submarine will also be exerted to lift forces due to hull bound vortexes which is described in Section 3.1. Even more complex, typically for 6 degrees of freedom systems, is combined movement, e.g., a pitching movement while yawing. In the case of submarines, these motions will be handled separately as suggested by [Fossen, 2011], that is, the model will not explicitly account for combined yaw and pitch movements.

[Feldman, 1979] proposes a way to model hull drag by applying strip theory, i.e., split the hull in multiple sections and then, the drag force on a section will be a function of the local velocity. For example the integral term in the Y_{HD}- expression with $w = 0$:

$$-\frac{\rho}{2} C_d \int_L h(x)(v + r \cdot x)|v + r \cdot x| dx \tag{4.12}$$

where $h(x)$ is the local hull height and L is the hull length. Correspondingly, the

yaw moment due to a turning motion will be:

$$-\frac{\rho}{2}C_d \int_L x \cdot h(x)(v + r \cdot x)|v + r \cdot x|dx \tag{4.13}$$

Hydrodynamics in literature

[Feldman, 1979] provides a complete notation and collection of the David W. Taylor naval ship research and development center standard equations of motion for submarines. These equations are widely quoted and referred to in submarine modelling papers and is, according to FOI[4]*, still the standard way of modelling underwater vehicles with six degrees of freedom. In addition to the hydrodynamic derivative terms, Feldman includes integral terms to model drag while turning and flow vortex lift effects. These equations will be extensively used in this thesis.*

[Humphreys and Watkinson, 1978] provides analytical expressions for approximating added mass terms. This is done by collecting work from [Lamb, 1932] and approximating the bare hull of a submarine as an ellipsoid. In addition, the paper includes semi-empirical added mass and inertia effects due to the flow around the hydroplanes. Finally, the validity and problems with the formulas are discussed.

[Ridley et al., 2003] uses a simplified version of Feldman's standard equations to simulate a torpedo. The coefficients are derived through physical model testing in a pool. From Feldman's equations the integral terms due to turning drag and hull vortexes are excluded. This is instead modeled by letting the force always be directed opposite to the inflow of the water with a drag coefficient that increases quadratically with the angle of attack and drift. The drag force is then divided into components in the different directions and will serve as drag when the model is turning, i.e., drifting.

[Watt, 2007] uses a CFD software to derive the hydrodynamic derivatives for a submarine computer model. However, he uses a distinct way of calculating the drag where coefficients are functions of the sway and heave drifts, e.g., the drag in x^R-direction:

$$X_D = X_{uvw}(u, v, w) \cdot (\sqrt{u^2 + v^2 + w^2})^2 \tag{4.14}$$

This is a way to model the change of flow around the hull while manoeuvring.

[Toxopeus, 2011] simulates a number of surface vessels with the hydrodynamic forces and moments computed through a CFD software, unlike the more common way of a coefficient based prediction. He finds that this is a more accurate approach in simulating water going vessels.

[Fossen, 2011] and [Fossen, 1994] are extensive works that collects a great deal of the current knowledge in the subject of hydrodynamics. The author compiles a number of different models that have been used in predicting ship motion through water over the years and refer to [Humphreys and Watkinson, 1978] for discussion and prediction of submarine hydrodynamic derivatives.

[4] Totalförsvarets forskningsinstitut, (Swedish defence research agency)

4.2 Generic submarine model

In this Section a model for a generic submarine will be derived. The equations in [Feldman, 1979] will serve as a template. The hydrodynamic added mass terms will be approximated according to [Humphreys and Watkinson, 1978].

As for the rudders, the equations proposed by [Toxopeus, 2011] will be used and modified for three dimensions and for the rotor propulsion and torque, the model in [Watt, 2007] will be used.

Hydrodynamic derivatives

The hydrodynamic derivatives will be calculated by approximating the submarine as an ellipsoid. The hydroplanes are seen as flat plates as suggested by [Humphreys and Watkinson, 1978]. The added mass effect from the sail will be calculated by approximating the sail as a huge hydroplane.

Cross flow drag

The *cross flow drag* was modelled according to [Feldman, 1979].

$$Y : -\frac{\rho}{2} C_d \int_L h(x) v(x) \sqrt{(w(x)^2 + v(x)^2)} dx \tag{4.15a}$$

$$Z : -\frac{\rho}{2} C_d \int_L b(x) w(x) \sqrt{(w(x)^2 + v(x)^2)} dx \tag{4.15b}$$

$$M : -\frac{\rho}{2} C_d \int_L x \cdot b(x) w(x) \sqrt{(w(x)^2 + v(x)^2)} dx \tag{4.15c}$$

$$N : -\frac{\rho}{2} C_d \int_L x \cdot h(x) v(x) \sqrt{(w(x)^2 + v(x)^2)} dx \tag{4.15d}$$

where $b(x)$ and $h(x)$ are the local width and heigh at x. $w(x)$ and $v(x)$ are the local velocities at x:

$$\begin{aligned} v(x) &= v + r \cdot x \\ w(x) &= w + q \cdot x \end{aligned} \tag{4.16}$$

C_d in (4.15) is the cross flow drag coefficient. For accurate prediction, C_d will have to be specified separately for each Equation in (4.15). Since the hull has different shape over the body, and the local velocities are different over the hull according to Equation (4.16), an even more accurate prediction will be to also let C_d be a function of the position x and the local velocity.

When specifying a submarine model, the functions $h(x)$ and $b(x)$ will have to be provided. When not specified, the model will use the value $C_d = 1.19$ for all equations in Equation (4.15) as suggested by [Hickey, 1990].

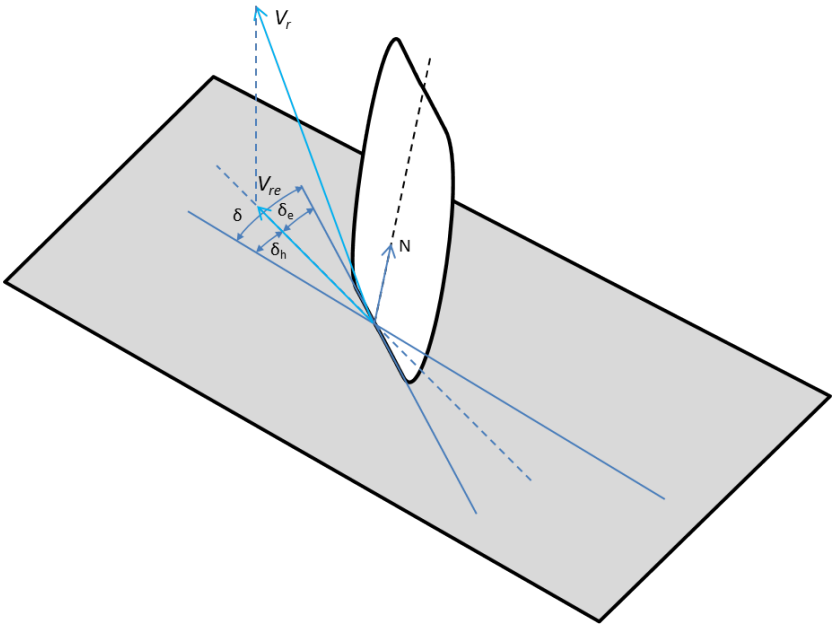

Figure 4.2: Rudder angles in three dimensions.

Control surfaces

[Toxopeus, 2011] presents formulas for rudder forces and moments for a surface going vessel. These equations, modified to fit three dimensions, will be presented in this section. As described in Section 3.1, the formulas need the hydrodynamic rudder angle δ_h.

The water velocity vector at a rudder at the position $\mathbf{x}_r$ (w/o hull and rotor effects) is calculated in Equation (4.17).

$$\mathbf{v}_r = -(\nu_1 + \nu_2 \times \mathbf{x}_r) \tag{4.17}$$

$$\begin{aligned} \nu_1 &= (u, v, w) \\ \nu_2 &= (p, q, r) \end{aligned} \tag{4.18}$$

This velocity will be projected on a plane orthogonal to the rudder, with normal $\mathbf{N}$, see Figure 4.2.

$$\mathbf{V}_{re} = (I - \frac{\mathbf{N}\mathbf{N}^\intercal}{\mathbf{N}^\intercal\mathbf{N}})\mathbf{V}_r{}^5 \tag{4.19}$$

Note that $\mathbf{V}_r$ and $\mathbf{v}_r$ is the same vector, only that $\mathbf{V}_r$ is the vector expressed as a column matrix. δ_h will be the angle between $\mathbf{V}_{re}$ and $[-1\ 0\ 0]^\intercal$. The drag and lift forces D_{ru} and L_{ru}, are calculated according to Section 3.1. The direction for D_{ru} will be the same as $\mathbf{V}_r$. L_{ru} will work in the direction $\mathbf{N}\times\mathbf{V}_r$.

Each hydroplane will have a specific direction in which it operates, i.e., a normal rudder could have the direction $(0,1,0)$ and a horizontal hydroplane could have the direction of operation $(0,0,1)$. As for an $\times$ configuration, the force directions could be $(0,\pm 1/\sqrt{2},\pm 1/\sqrt{2})$. Apart from that, the user will have to specify the hydroplane positions $\mathbf{x}_{hp1-6}$, the hydroplane area and the lift and drag coefficients C_l and C_d. With this data, the lift and drag forces and moments for each hydroplane are calculated.

An issue with the equations presented by [Toxopeus, 2011], is that they do not deal with cross flow and coupled motion in 3 dimensions. For a $+$ rudder configuration and no combined pitch/yaw motion, this would not be a problem. But for $\times$ rudder configurations, the rudders will experience coupled motion even when combined pitch/yaw motion is avoided.

Tower drag and lift

An attempt to model the tower lift and drag was done by using the same equations as for the hydroplanes, applied to the tower dimension and position. It is difficult to study the validity of this method. The only validation performed, was to study the directions of the forces, but not the magnitude. This suggest that this approximation should not be used in a simulation before this method is verified. This will not be further discussed.

Propeller propulsion and force

Equations for forces and torques created by the propeller, were presented in Section 3.1, where X_P and K_P depend on the coefficients K_t and K_q, which in turn are functions of the advance ration J. These two coefficients depend heavily on the shape of the propeller and have to be derived through actual testing or CFD calculations, which is outside the scope of this thesis. As for the generic model, the user has to specify how K_t and K_q are functions of J. However, the model will provide a suggested relation according to previous works.

[Watt, 2007] presents two eighth-order polynomial interpolations for K_t and K_q as functions of the advance ratio J, derived through CFD calculations. Other relations have been derived, e.g., by [Toxopeus, 2011], but [Watt, 2007] also deals with the subject of submarines, hence, this was chosen. The coefficients K_t and K_q as functions of the RPS n at two different speeds are plotted in Figure 4.3. The interpolating polynomials can be found in Appendix A.1. The reader will probably notice the RPS n in the denominator for the advance ratio, this function is therefore not valid for close to zero RPS. At some points, K_t and K_q are negative, which mean that the force/torque from the propeller is negative, which of course is not at all impossible, since slow RPS at high velocities could produce more drag than propulsion.

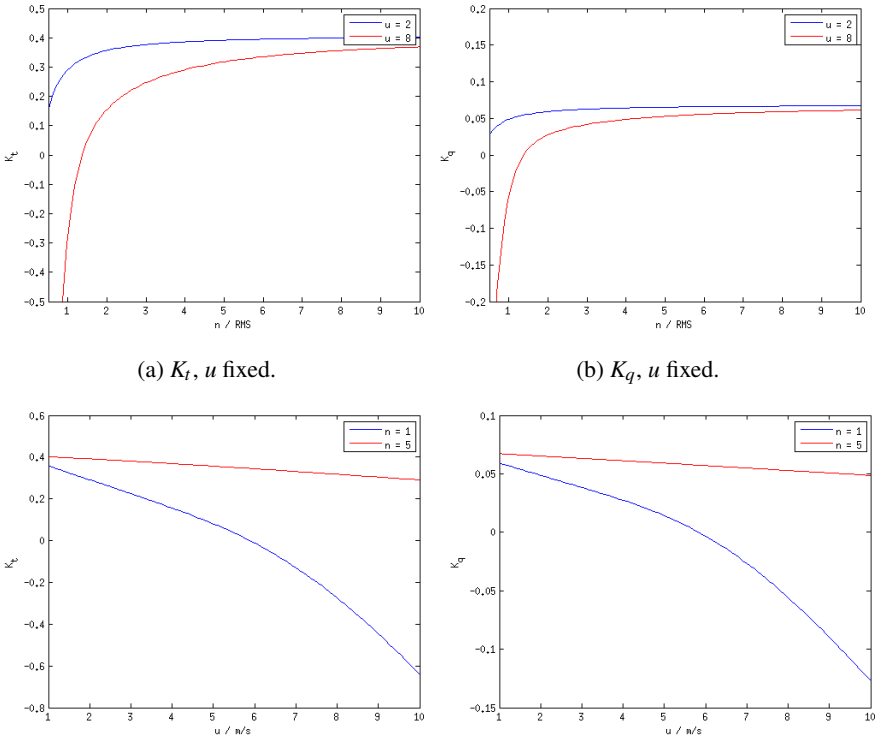

(a) K_t, u fixed.

(b) K_q, u fixed.

(c) K_t, n fixed.

(d) K_q, n fixed.

Figure 4.3: $K_t(J)$ and $K_q(J)$ relation.

Hydroplane dynamics

The submarine model is manoeuvred by slanting the hydroplanes, i.e., specifying mechanical angles δ_k. However, positioning the hydroplanes are control problems themselves. An accurate dynamic model description for the different hydroplanes is outside the scope of this thesis, although it could be desirable to include some hydroplane dynamics.

For the generic model, the positioning of the hydroplanes is approximated by a simple first order system where it is possible for the user to specify a time constant for each control surface.

$$\delta_k = \frac{1}{s/T_k + 1}\delta_{refk} \tag{4.20}$$

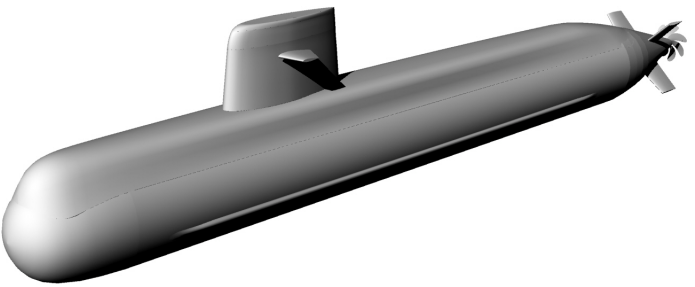

Figure 4.4: Submarine demo model.

Rotor dynamics

Similarly to the hydroplanes, the rotor dynamics is approximated by a simple first order system with a user defined time constant.

$$n = \frac{1}{s/T + 1} n_{ref} \tag{4.21}$$

4.3 Submarine demo model

During the literature study for this thesis, the authors came into contact with FOI. They confirmed the difficulties in modelling water crafts but provided a full model of a demo submarine derived through CFD calculations of a CAD model of a submarine (Figure 4.4). The mathematical model was according to Feldman's equations. Table 4.1 shows the mechanical data for the demo submarine. The complete set of hydrodynamic coefficients can be found Section 6.1, and compared with the coefficient derived from mechanical data according to the approximation method by [Humphreys and Watkinson, 1978].

General features of the demo model Some general features of the demo submarine are presented in the list below.

[6] Relative the aft of the submarine, expressed a as positive oriented orthonormal coordinate system (x, y, z) with z- axis upwards.

	unit	data
surfaced mass	[kg]	$1942.3 \cdot 10^3$
submerged mass	[kg]	$1942.3 \cdot 10^3$
I_x	[kg·m^2]	$1.3 \cdot 10^7$
I_y	"	$43.7 \cdot 10^7$
I_z	"	$43.2 \cdot 10^7$
I_{xy}	"	$-99 \cdot 10^3$
I_{zx}	"	$-7478 \cdot 10^3$
I_{yz}	"	$-56 \cdot 10^3$
L (length)	[m]	6.23
max height	[m]	11.9
max with	[m]	6.20
rotor diameter	[m]	3.40
aft HP area	[m^2]	6.08
tower HP area	[m^2]	3.41
$\mathbf{x}_G{}^6$	[m]	$(32.61, 0.000, -0.067)$
$\mathbf{x}_B$	[m]	$(32.61, 0.000, 0.136)$

Table 4.1: Main data of the demo submarine.

- The submarine has tower hydroplanes instead of bow hydroplanes.
- The submarine has $\times$ aft rudder configuration.
- No propulsion was modeled by FOI, instead the method described in Section 4.2 will be used.
- Rudder forces have a linear relation to the rudder angles, except for drag in x^R direction which will have a quadratic relation, according to Feldman's equations.
- Rudder forces have a quadratic relation to the forward speed u, as is also according to Feldman's equation.

The aft hydroplanes are numbered as: 1- upper starboard, 2- lower starboard, 3- lower port, and 4- upper port. The mechanical rudder angles are oriented such that a positive rudder angle results in a positive roll moment.

4.4 Control design

The submarine demo model was chosen to be the final model for which an autopilot were designed.

This section does not present numbers or controller parameters, but rather a thorough explanation of the controller design.

Model IOs

The control signals to the submarine at the current state[7] are the requested hydroplane positions and rotor RMS. The outputs are the signals measured by the INS and the control efforts, i.e. actual hydroplane positions and rotor RMS, see Figure 4.5. The possibility to view the true states of the process will also exist for validation purposes.

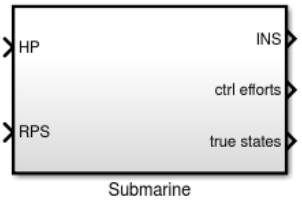

Figure 4.5: Submarine simulator IOs.

Controller task

With the controller requirements from Section 1.4, the final system should take the form as in Figure 4.6. Since there are no requirements for velocity control, this will not be included in this thesis, i.e., the control system's means to actuate the submarine will be through the hydroplanes.

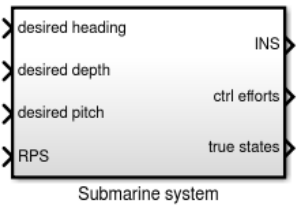

Figure 4.6: Simulator system IOs.

Controller hierarchy

The submarine has a number of different modes, but not all are required to follow a reference. When linearized, the system was chosen to have the states $\bar{\mathbf{x}}$ in Equation 4.22.

$$\bar{\mathbf{x}} = [\phi\ \theta\ \delta_1\ \delta_2\ \delta_3\ \delta_4\ \delta_5\ \delta_6\ u\ v\ w\ p\ q\ r]^\mathsf{T} \tag{4.22}$$

[7] Future work could include including the condition of the different tanks as control signals.

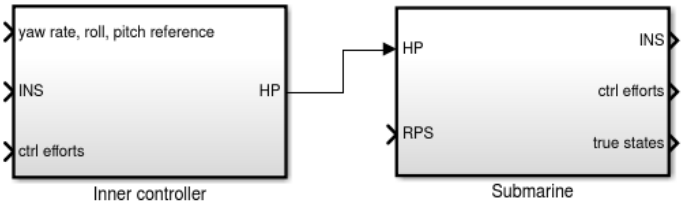

Figure 4.7: r, ϕ, θ controller.

Depth and heading are not included in the state vector. They do however have a dynamic relation to the state vector. With zero roll ($\phi = 0$), the change in depth can be expressed as $\dot{z} = w - u \cdot sin(\theta)$. In a sledge mode depth changing manoeuvre, w is not accounted for, and for small θ the equation falls down to a first order integrator at a certain speed (u constant):

$$\dot{z} = u \cdot \theta \tag{4.23}$$

As for the elevator depth changing manoeuvre, the pitch will stay zero and the relation becomes instead:

$$\dot{z} = w \tag{4.24}$$

With zero roll and pitch, the change in yaw will also be of first order integrator characteristics, $\dot{\psi} = r$. The natural choice for a controller structure would then be to, at first, stabilize and control ϕ, θ, and r (Figure 4.7). With this, controlling the depth and yaw becomes a simple task.

Inner controller

The inner loop r, ϕ, θ-controller was chosen to be of LQ[8] state feedback characteristic. An integrator for each controlled mode was added to remove stationary errors caused by simulated stationary disturbances and model inaccuracies due to the linearization. The system on state space form becomes, with the notation in 3.3, as in Equation (4.25).

$$\begin{aligned} \dot{\bar{\mathbf{x}}} &= \mathbf{A}\bar{\mathbf{x}} + \mathbf{B}\delta_{ref} \\ \mathbf{z} = \mathbf{M}\bar{\mathbf{x}} &= \begin{bmatrix} 0 & 0 & 0 & \cdots & 0 & 1 \\ 1 & 0 & 0 & \cdots & 0 & 0 \\ 0 & 1 & 0 & \cdots & 0 & 0 \end{bmatrix} \bar{\mathbf{x}} \end{aligned} \tag{4.25}$$

In order to allow state feedback, an observer had to be added since only the INS and control effort signals can be measured. The final inner loop control structure can be found in Figure 4.8.

[8] *Linear Quadratic Control*, i.e., linear system with quadratic criteria

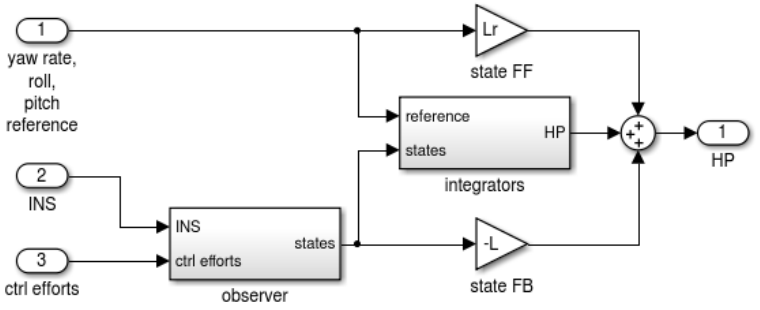

Figure 4.8: Inner loop controller structure.

State feedback The state feedback gain $\mathbf{L}$ was calculated with the Matlab command $lqry(sys, \mathbf{Q}, \mathbf{R}, \mathbf{N})$, which computes the optimal state feedback controller of system *sys* with the weight function, see Section 3.3:

$$J = \mathbf{z}^\intercal \mathbf{Q}\, \mathbf{z} + \delta_{ref}^\intercal \mathbf{R}\, \delta_{ref} + \mathbf{z}^\intercal \mathbf{N}\, \delta_{ref} \tag{4.26}$$

State feed forward The feed forward gain $\mathbf{L}_r$ is given by Equation 3.3

$$[\mathbf{M}(\mathbf{BL} - \mathbf{A})\mathbf{B}] \cdot \mathbf{L}_r = \mathbf{I}_{3\times 3} \tag{4.27}$$

$\mathbf{M}(\mathbf{BL}-\mathbf{A})\mathbf{B}$ has the size 3×6, and $\mathbf{L}_r$ the size 6×3. Equation (4.27) is therefore an underdetermined system of equations, i.e., we have a total of 18 unknown variables but only 9 equations. This was expected, since there are more than one way to operate the hydroplanes to create a certain movement. In addition to this, a change in roll reference will probably never occur. This means that the second column in $\mathbf{L}_r$ is of no interest. The second row of $\mathbf{M}(\mathbf{BL}-\mathbf{A})\mathbf{B}$ and the second column of $\mathbf{L}_r$ are therefore removed, and form Γ and $\hat{\mathbf{L}}_r$.

$$\Gamma \cdot \hat{\mathbf{L}}_r = \mathbf{I}_{2\times 2} \tag{4.28}$$

The result is a system of equations with 12 unknown variables but only 4 equations. This meant that it was possible to add more constraints on the solution. To begin with, there is no need for the bow/tower hydroplanes to answer to a reference change in r, which means $\hat{\mathbf{L}}_{r5,1} = \hat{\mathbf{L}}_{r6,1} = 0$. The bow/tower HPs are also often connected, i.e., $\hat{\mathbf{L}}_{r6,2} = \hat{\mathbf{L}}_{r5,2}$. Equation (4.28) becomes:

$$\Gamma \cdot \begin{bmatrix} \hat{\mathbf{L}}_{r1,1} & \hat{\mathbf{L}}_{r1,2} \\ \hat{\mathbf{L}}_{r2,1} & \hat{\mathbf{L}}_{r2,2} \\ \hat{\mathbf{L}}_{r3,1} & \hat{\mathbf{L}}_{r3,2} \\ \hat{\mathbf{L}}_{r4,1} & \hat{\mathbf{L}}_{r4,2} \\ 0 & \hat{\mathbf{L}}_{r5,2} \\ 0 & \hat{\mathbf{L}}_{r5,2} \end{bmatrix} = \begin{bmatrix} 1 & 0 \\ 0 & 1 \end{bmatrix} \tag{4.29}$$

Equation (4.29) is still an underdetermined system of equations. Consider instead the optimization problem of solving (4.29) with the least possible control effort. The HP angles δ at a reference change relate to the values in $\mathbf{L}_r$. With $\hat{\mathbf{L}}_r = [\hat{\mathbf{L}}_{r1}\ \hat{\mathbf{L}}_{r2}]$, $\mathbf{X} = \begin{bmatrix} \hat{\mathbf{L}}_{r1} \\ \hat{\mathbf{L}}_{r2} \end{bmatrix}$ is defined.

$$\begin{aligned} \min_{\mathbf{X}} \quad & \mathbf{X}^\mathsf{T}\mathbf{H}\mathbf{X} \\ \text{s.t.} \quad & \Gamma \cdot \hat{\mathbf{L}}_r = \mathbf{I}_{2\times 2} \end{aligned} \tag{4.30}$$

With $\mathbf{H}$ in Equation (4.30) it is possible to weigh certain HPs, to create the desired reference tracking control. It is also possible to add additional constraints to the problem (4.30), e.g., if one hydroplane has malfunctioned it is possible to add this as a constraint to the optimization problem.

Observer The state feedback controller requires the state vector $\bar{\mathbf{x}} = [\phi\ \theta\ \delta_1\ \delta_2\ \delta_3\ \delta_4\ \delta_5\ \delta_6\ u\ v\ w\ p\ q\ r]^\mathsf{T}$. From Section 1.1 the measured states could include $\mathbf{y} = [\phi\ \theta\ \delta_1\ \delta_2\ \delta_3\ \delta_4\ \delta_5\ \delta_6\ u\ p\ q\ r]^\mathsf{T}$. However, as for u, the observer would naturally believe that u is constantly decreasing due to the rotor RPS is not included as a model actuator. This would probably result in a stationary error in the log velocity u. To counter this, a new system model was derived for the observer where the rotor RPS was included as a system actuator together with the hydroplane angles. To simplify the observer, the *actual* hydroplane angles and rotor RPS served as the input signals since they were all measurable. This resulted in the state space system in Equation (4.31) for the observer with the states $\bar{\mathbf{x}}' = [\phi\ \theta\ u\ v\ w\ p\ q\ r]$, and system matrices $\mathbf{A}'$, $\mathbf{B}'$, and $\mathbf{C}'$.

$$\begin{aligned} \dot{\bar{\mathbf{x}}}' &= \mathbf{A}'\bar{\mathbf{x}}' + \mathbf{B}' \begin{bmatrix} \delta \\ n \end{bmatrix} \\ \mathbf{y}' &= \begin{bmatrix} \mathbf{I}_{3\times 3} & \mathbf{0}_{3\times 2} & \mathbf{0}_{3\times 3} \\ \mathbf{0}_{3\times 3} & \mathbf{0}_{3\times 2} & \mathbf{I}_{3\times 3} \end{bmatrix} \bar{\mathbf{x}}' \end{aligned} \tag{4.31}$$

with:

$$\bar{\mathbf{x}} = \begin{bmatrix} \mathbf{y}'_1 & \mathbf{y}'_2 & \delta^\mathsf{T} & \mathbf{y}'_3 & \cdots & \mathbf{y}'_8 \end{bmatrix}^\mathsf{T} \tag{4.32}$$

A Kalman filter was used to estimate the states in Equation (4.31). Assume that model disturbances and measurement noise η_1 and η_2 act on the system (4.31) as $\dot{\bar{\mathbf{x}}}' = \ldots + \mathbf{N}\eta_1$ and $\mathbf{y}' = \ldots + \eta_2$. η_1 was chosen to be external force and torques. Hence, $\mathbf{N} \approx \mathbf{M}^{-1}$. If it is necessary to account for model inaccuracies due to linearization of a nonlinear model in the Kalman filter, it too has to be included in the correlation matrix for η_1.

Integrators The integrators simply continuously integrate the control errors in r, ϕ, and θ. These are added to the controller output after being multiplied by tuning constants. According to the hydroplane orientation in Section 4.3, the integrators will be added to the HP angles as in Figure 4.9.

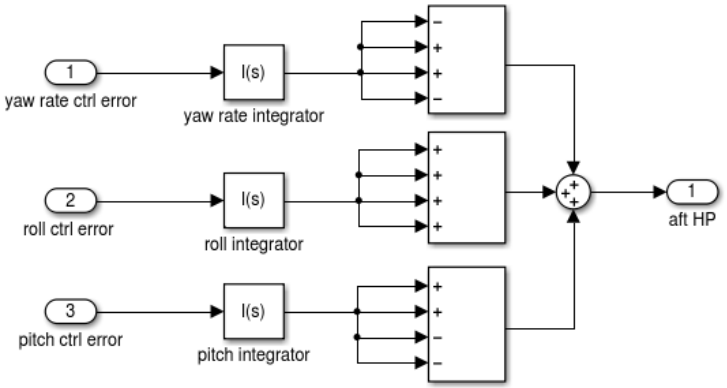

Figure 4.9: Integrator signs.

Heave controller

The inner control loop does not include elevator mode control since it only allow references in r, ϕ, and θ. Another controller was added parallel to the inner controller for this purpose, named the *heave controller*, see Figure 4.10. In an elevator mode manoeuvre, this controller use the tower HP to heave the submarine, i.e., change the depth. Meanwhile, the pitch reference is kept zero and the inner controller will work to keep the submarine at zero pitch.

Controller type The heave controller was chosen to be of PID type with control signal saturation and integrator anti-windup. To improve performance, a second order prefilter $F(s)$ was added to smooth out reference steps.

$$F(s) = \frac{5}{s^2 + 20s + 5} \tag{4.33}$$

Reference saturation A linear system with a linear controller acting on different reference changes will scale the controller effort linear with the reference changes. That is, let $u(t)$ be the initial controller output from a reference change $r(t)$. If the reference change is scaled by a constant C, i.e., $r_2(t) = C \cdot r(t)$, the control effort will be $u_2(t) = C \cdot u(t)$.

For a submarine, as for many other practical control problems, it is not possible to always linearly scale the controller effort with the reference change, due to actuator saturations[9]. With anti-windup properly implemented on the controller I part, this does not have to be a problem. But the submarine autopilot should be able to answer to a wide range of reference changes, e.g., a depth change of a few meters to perhaps 200m, both which should be performed in a similar manoeuvre.

[9] In the case of submarines, the hydroplanes angles have a mechanical limit.

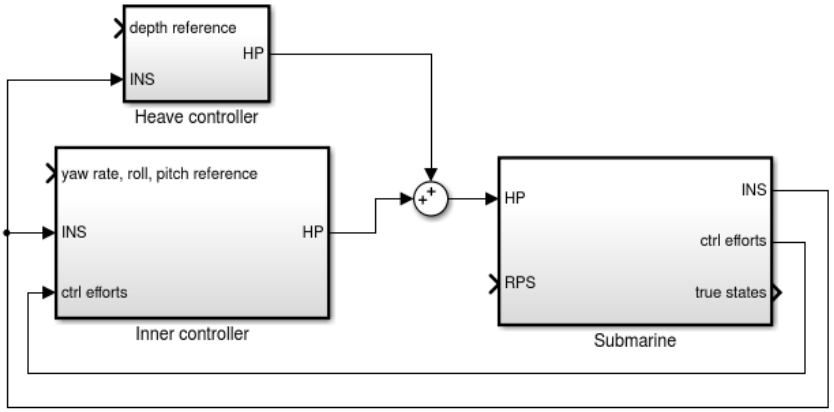

Figure 4.10: Heave controller in parallel with the inner controller.

Assume a submarine in an elevator depth changing mode. In the case of a huge reference change, the P part in a PID controller would immediately saturate the tower hydroplanes. Compare this to a lower reference change, low enough for the P part to not saturate the hydroplanes. Perhaps the integrator part will saturate the hydroplanes after some time, but in either case, the responses will initially look different.

In Figure 4.11, a system is simulated with with two different reference steps. The saturation on the control effort is 1. As can be seen, the control effort with the larger step is immediately saturated while for the smaller, it is saturated only after some time. This effect will show up when changing submarine depth in an elevating fashion. In order to make the two step responses look more alike, a saturation on the control error was added for the depth. The PID was tuned for a certain step response, e.g., 10m, and then the control error was saturated to not make larger steps then that, i.e., $\pm$10m, see Figure 4.12. Two different step responses will now look somewhat alike, apart from that that the big reference step (blue line in Figure 4.11) will raise further than the small step (red), before flattening out. This will make depth changing look something like in Figure 4.13.

Gain scheduling

According to the controller task in Section 1.4, the controller was chosen to include three different modes for different regions of velocity (Figure 4.14), with borders 6 and 13 knots. To avoid back and forth switching close to a border, a hysteresis on 0.3 m/s was added. Controller options are found in Table 4.2.

Three different controllers were derived, one for each velocity region. Since the submarine has quadratic dynamics, the controllers were designed at the velocities 3, 6 and 8 m/s, i.e., in the upper half of the regions. Due of the quadratic behaviour,

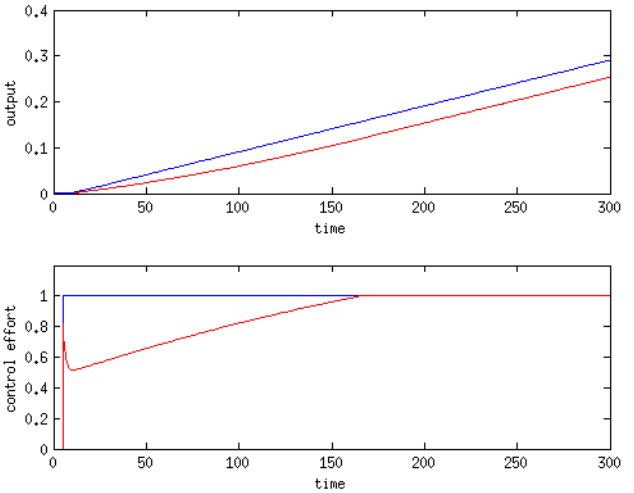

Figure 4.11: Simulated output from the same control system with different reference step. Blue: large step, red: smaller step

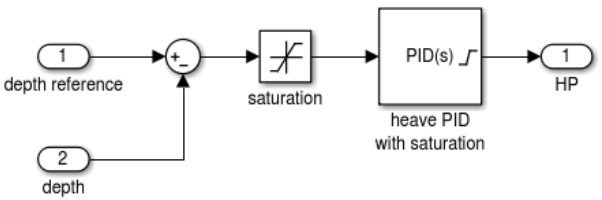

Figure 4.12: Control error saturation.

the *dynamic mean* in each region should be at a velocity closer to the upper end of each region.

Integrators To achieve bumpless control, the integrators had to include tracking (see Section 3.3), i.e., the non-active integrators will follow the output of the active one.

Observers In order to allow different observers for the three different regions, it is possible to individually activate and deactivate the observers. The switching should be performed with minimal bump, hence, the output from the last active observer serves as an initial state to the activated one.

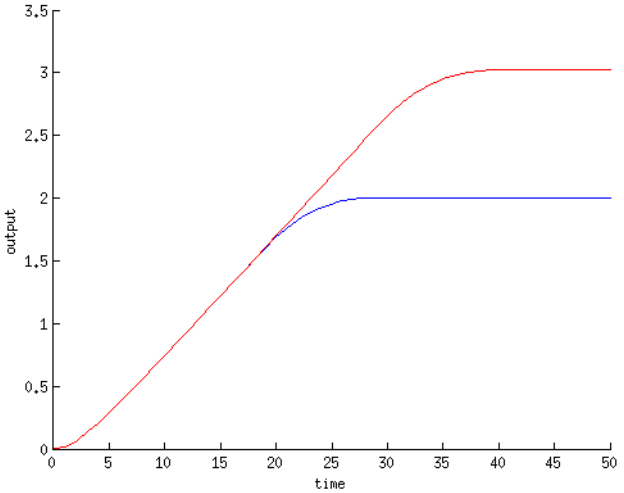

Figure 4.13: Step response with control error saturation.

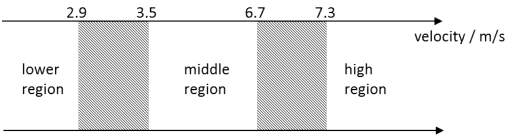

Figure 4.14: Velocity regions, the shaded part is the hysteresis.

region	1	2	3
tower HP	on	on	off
depth k. mode	elevator mode	elevator mode	sledge mode
depth c. mode	"	sledge mode	"

Table 4.2: Controller features in the regions.

State FF and FB The submarine was numerically linearized at the three different velocities (3, 6, and 8m/s). State FB gains were derived with different weighting matrices.

As for the lower region, the tower HP are used to elevate the submarine in depth changing and depth keeping manoeuvres which are not explicitly accounted for in the state FF and FB. The tower HP were hence greatly weighted in order to

minimize interference between the controllers, i.e., the FB should not use the tower HP to control the pitch since they are extensively used by the heave controller. As for the state FF in the low velocity region, the tower HP angle $= 0$ was a condition to the optimisation.

The medium velocity region features a combined elevator and sledge depth changing mode. Depth changing manoeuvres are performed in sledge mode, while depth keeping are performed in elevator mode. Here the tower HP are weighted less compared to the low and high velocity regions.

In the high velocity region, again, the tower hydroplanes are heavily weighted even though they are not used by another parallel controller. This is to satisfy the controller task in Section 1.4. To keep the tower HP mechanical angle zero was a condition to the FF optimization, as in the lower region.

Since the state FB and FF gains are different in the regions, the controller will suffer a slight bump at the moment of the switch.

Outer loop

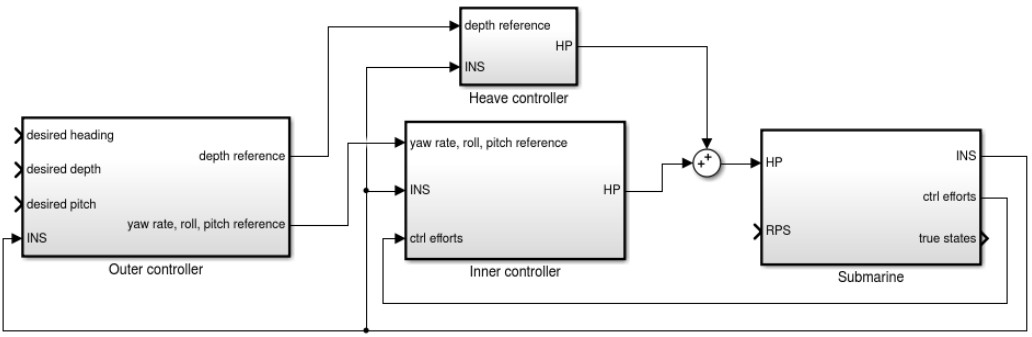

Figure 4.15: Inner and outer loop control.

The outer loop controller will be the interface between depth, pitch, and heading references from the operator, and yaw rate, pitch, and roll references to the inner loop controller. It is integrated in the control system as shown in Figure 4.15. The outer controller will see the inner loop, as simple first order integrators K/s as explained in Section 4.4. First order integrator control, can be achieved by simple P controller. However, the inner loop can only be seen as first order integrators below its bandwidth ω_B. This gives us a fundamental limitation on the speed of the closed outer loop, i.e., $P \cdot K << \omega_B$ (Figure 4.16).

Heading control Figure 4.17 shows the structure for the outer loop heading controller. It is of simple P characteristic with a saturation to avoid huge r reference signals. The saturation is dynamic, i.e., different in each velocity region, higher speeds allow higher yaw rate r.

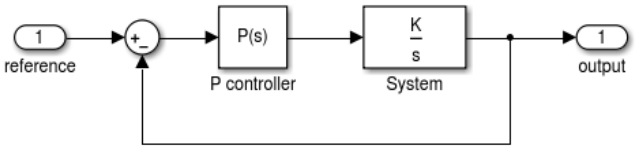

(a) Integration system with P controller.

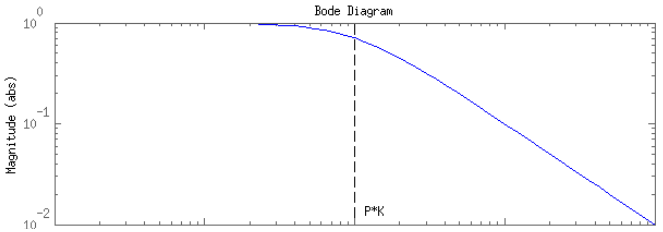

(b) Closed loop bode diagram.

Figure 4.16: Integrator controller bandwidth.

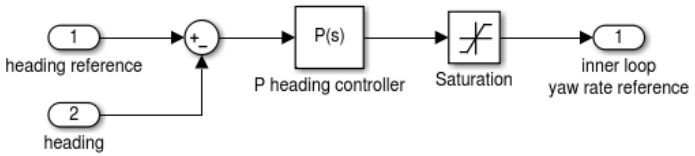

Figure 4.17: Outer loop heading controller structure.

The heading measurement from the INS is in the interval $0-360°$. Such a non-linearity will cause control problems. Assume that the current heading is 10° and a new reference is given to 350°. The favourable choice of turning, is of course to steer port 20°, but the controller will steer the submarine the other way. Instead, if the new reference should be $-10°$, the submarine will turn to port, but will not stop at 350°. The heading from the INS will therefore be *unwrapped* from the interval $[0,360)$ and instead $\in \mathbb{R}$. This means that if the submarine has started facing north, spun around two turns to end up facing north again, this unwrapped heading will be 720°. With this, in the example above, the reference signal can indeed be -10° and the submarine heading will end at 350° (unwrapped heading will be -10°).

It is now a simple task to perform different turning manoeuvres, e.g., if the submarine should make the shortest turn, longest turn, make the turn port/starboard, etc. Assume that the current unwrapped heading is 730° (INS heading is 10°) and a new heading reference is given to face east (wrapped heading ref 90°). If the submarine should take the closest path, the new unwrapped heading reference will

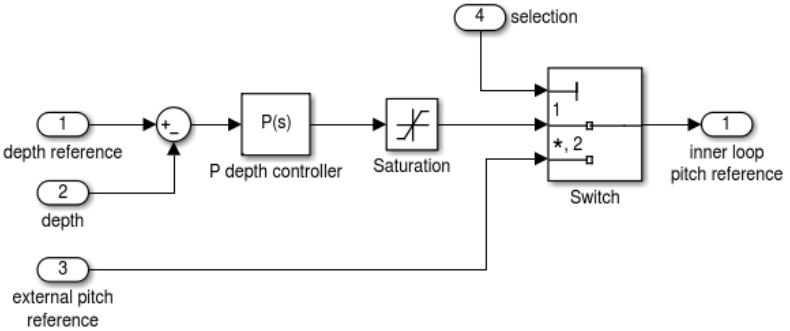

Figure 4.18: Outer loop depth control structure.

be $720° + 90° = 810°$. To make the submarine take the longer way the reference should be set to $720° - 270° = 450°$ etc.

Depth control The depth controller (Figure 4.18) will provide a pitch reference to the inner loop in the high velocity region and, while in depth changing mode, in the medium velocity region. While in depth keeping mode (medium velocity region) and in the low velocity region, the heave controller will control the depth, hence, the pitch reference to the inner controller, will be the external pitch reference from the operator (at most times zero). The *selection* input block in Figure 4.18 will choose if the operator pitch reference shall be passed to the inner loop, or the pitch reference from the outer loop depth controller, in the latter case the heave controller should not operate. This selection will also be a part of the outer loop controller. A control signal saturation is added to avoid huge pitch references to be passed to the inner loop controller.

Controller enabling and resetting The outer loop controller is a more sophisticated controller than the inner loop controller. It does more logical decisions, e.g., determines the current velocity region and switches between depth keeping/changing mode. To accomplish this, it needs the possibility to turn off the heave controller. The inner loop and heave controller therefore need to support more utilities in form of switching (between regions) and integrator enabling/disabling and reset. To simplify, all integrators/PIDs are reset when disabled.

- All the integrator are disabled (and reset) during a corresponding manoeuvre, i.e., the pitch integrator is disabled during a sledge depth changing motion and the yaw rate integrator is disabled when initiating a heading change. The roll reference is always zero, hence the roll integrator will not be disabled due to a reference change.
- All integrators are disabled when the corresponding control effort is higher than a certain threshold, e.g., 90% of the maximum control effort.

- The heave PID is disabled when in:
    1. sledge mode in the medium region
    2. high velocity region

Outer loop controller structure Figure 4.19 shows the complete structure for the outer loop. The different part will be summarized in the list below.

- *determine velocity region*. This block simply determines which is the current velocity region according to Figure 4.14.
- *determine manoeuvring*. If a new reference larger than a certain threshold has been given, this block sets *manoeuvring* to *true*. Observe, *manoeuvring* is a vector with two elements for heading and depth respectively. *manoeuvring* is set to false when nearing the reference.
- *determine mode*. This block determines if the submarine currently should move in a sledge or elevating fashion. Naturally, it needs the region and if the submarine is in a manoeuvre.

  When in the low velocity region, as seen in Table 4.2, the submarine controller will always stay in elevator mode.

  In the medium velocity region, the submarine will be in elevator mode when *manoeuvre* is false and switch to sledge mode, when *manoeuvre* turns true.

  In the high velocity region, sledge mode is always chosen.
- *P controllers*. This block contains the P controllers for depth and heading.
- *controller enable/ disable*. This block turns on/off the heave PID and the inner loop controller integrators.

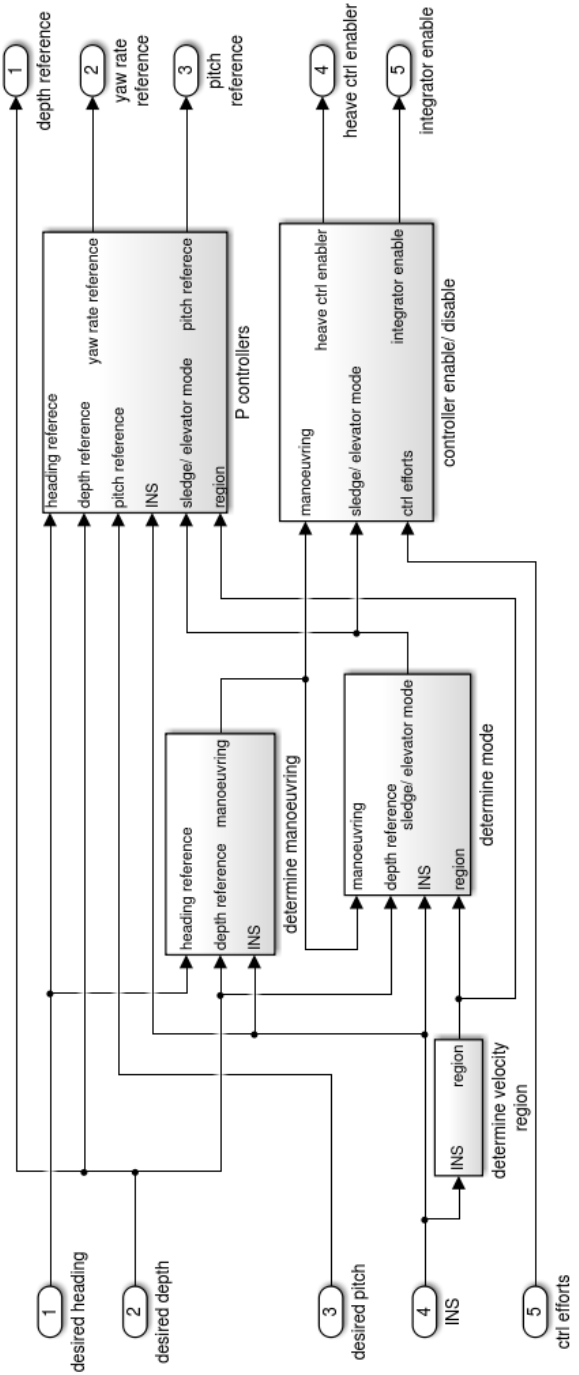

Figure 4.19: Outer loop controller structure.

5

Results

5.1 Time constants and saturations

This is a collection of the time constants and submarine actuator saturations, that was used in the submarine simulator.

- Time constants for all the hydroplane was chosen to 3s.
- Time constant for the rotor was chosen to 6s.
- Hydroplane angle saturation was chosen to $\pm 30°$.
- Rotor RPS was saturated to $[0.6, 2.4]$/s to fit the velocity interval 4- 16 knots.

5.2 Final controller

Inner loop controller

State FB The state feedback gain was calculated with the weights for the different regions as presented in Table 5.1.

State FF Table 5.2 displays the weights and conditions used to calculate the feed-forward gain $\mathbf{L}_r$ in the three regions, see Section 4.4 for information how this was calculated.

region	1	2	3
Q	$\begin{bmatrix} 500 & 0 & 0 \\ 0 & 10 & 0 \\ 0 & 0 & 10 \end{bmatrix}$	$\begin{bmatrix} 100 & 0 & 0 \\ 0 & 10 & 0 \\ 0 & 0 & 10 \end{bmatrix}$	$\begin{bmatrix} 100 & 0 & 0 \\ 0 & 10 & 0 \\ 0 & 0 & 10 \end{bmatrix}$
R	$\begin{bmatrix} 0.1 & 0 & 0 & 0 & 0 & 0 \\ 0 & 0.1 & 0 & 0 & 0 & 0 \\ 0 & 0 & 0.1 & 0 & 0 & 0 \\ 0 & 0 & 0 & 0.1 & 0 & 0 \\ 0 & 0 & 0 & 0 & 1.0 & 0 \\ 0 & 0 & 0 & 0 & 0 & 1.0 \end{bmatrix}$	$\begin{bmatrix} 0.1 & 0 & 0 & 0 & 0 & 0 \\ 0 & 0.1 & 0 & 0 & 0 & 0 \\ 0 & 0 & 0.1 & 0 & 0 & 0 \\ 0 & 0 & 0 & 0.1 & 0 & 0 \\ 0 & 0 & 0 & 0 & 1.0 & 0 \\ 0 & 0 & 0 & 0 & 0 & 1.0 \end{bmatrix}$	$\begin{bmatrix} 0.1 & 0 & 0 & 0 & 0 & 0 \\ 0 & 0.1 & 0 & 0 & 0 & 0 \\ 0 & 0 & 0.1 & 0 & 0 & 0 \\ 0 & 0 & 0 & 0.1 & 0 & 0 \\ 0 & 0 & 0 & 0 & 10 & 0 \\ 0 & 0 & 0 & 0 & 0 & 10 \end{bmatrix}$

Table 5.1: State FB weights.

region	1	2	3
tower HP conditions	off	does respond to reference in θ	off
H	$\begin{bmatrix} 1&0&0&0&0&0&0&0&0&0&0&0 \\ 0&1&0&0&0&0&0&0&0&0&0&0 \\ 0&0&1&0&0&0&0&0&0&0&0&0 \\ 0&0&0&1&0&0&0&0&0&0&0&0 \\ 0&0&0&0&-&0&0&0&0&0&0&0 \\ 0&0&0&0&0&-&0&0&0&0&0&0 \\ 0&0&0&0&0&0&1&0&0&0&0&0 \\ 0&0&0&0&0&0&0&1&0&0&0&0 \\ 0&0&0&0&0&0&0&0&1&0&0&0 \\ 0&0&0&0&0&0&0&0&0&1&0&0 \\ 0&0&0&0&0&0&0&0&0&0&50&0 \\ 0&0&0&0&0&0&0&0&0&0&0&50 \end{bmatrix}$	"	"

Table 5.2: State FF weights and conditions.

Integrators The numerical values will not be presented, see Section 4.4 for information about the integrators. The integrators were implemented in discrete time as mentioned in Section 2.2.

Observer The observer was also implemented in discrete time by sampling the linearized model. The observer gains were then calculated with white noise intensities presented in Equation (5.1).

$$E(\eta_1 \cdot \eta_1^\intercal) = \begin{bmatrix} 10^4 & 0 & 0 & 0 & 0 & 0 \\ 0 & 10^4 & 0 & 0 & 0 & 0 \\ 0 & 0 & 10^4 & 0 & 0 & 0 \\ 0 & 0 & 0 & 10^6 & 0 & 0 \\ 0 & 0 & 0 & 0 & 10^6 & 0 \\ 0 & 0 & 0 & 0 & 0 & 10^6 \end{bmatrix}$$
$$E(\eta_2 \cdot \eta_2^\intercal) = \begin{bmatrix} 10^{-13} & 0 & 0 & 0 & 0 & 0 \\ 0 & 10^{-13} & 0 & 0 & 0 & 0 \\ 0 & 0 & 10^{-11} & 0 & 0 & 0 \\ 0 & 0 & 0 & 10^{-12} & 0 & 0 \\ 0 & 0 & 0 & 0 & 10^{-12} & 0 \\ 0 & 0 & 0 & 0 & 0 & 10^{-12} \end{bmatrix} \tag{5.1}$$

Heave controller

Again, the authors see no point in presenting the numerical values of the PID controller. As for the control error saturation, it was chosen to $\pm$5m. The output from the PID saturated at $\pm 20^\circ$. Also the heave controller was a discrete controller.

Outer loop controller

Saturations As mentioned in Section 4.4 the P controllers for references in r and θ to the inner loop were saturated to avoid huge reference signals. The final results from these are presented in Table 5.3.

Switching To summarize, the conditions for the different outputs from the block in Figure 4.19 are presented in Table 5.4.

section	1	2	3
r	$\pm 0.6^\circ/\text{s}$	$\pm 1.2^\circ/\text{s}$	$\pm 3^\circ/\text{s}$
θ	$\pm 15^\circ$	$\pm 15^\circ$	$\pm 15^\circ$

Table 5.3: Outer loop controller saturations.

5.3 Simulation plots

In this Section, a number of plots from different simulated manoeuvres will be presented to verify that the control system works as intended. Three different test manoeuvres will be presented along with some of the most interesting plots.

When control efforts are plotted, they are normalized to be a percentage of the maximum control effort, i.e., fit in the interval $[-1, 1]$. For example, the roll effort is 1 if all the rudder are saturated to maximum positive angle, see rudder orientation for the demo submarine in Section 4.3.

Test Case One

The first manoeuvre will be testing reference changes in heading and depth. This test will be performed in the middle velocity region, around 6 m/s. The first change in reference will be a change in heading, 90° starboard followed by 90° port. After stabilizing, a reference change in depth will be performed, starting at a depth of 100m. First the submarine will dive to 120m, and then ascend to 80m. The results of the simulation are presented in Figures 5.1-5.4.

Heading Change As seen in Figure 5.1, a heading change of 90° takes approximately 120 seconds in the current mode. This might not seem very fast, but as seen in Figure 5.4, the yaw effort is relatively low, which means that a faster turn is possible. It can also be seen in Figure 5.3 that the submarine will pitch slightly positive when initiating the turn. Real submarines do also have a tendency to lower their afts when turning[1]. Figure 5.4 proves that the control system compensates for this.

Depth Change Figure 5.2 displays the depth. During the veer (0-500s), the depth alters slightly, which of course is an effect of the pitching motion. As seen in the figure, a change of reference in depth of 20m as well as 40m takes approximately the same time. According to Table 5.3, the pitch reference from the outer controller is saturated at $\pm 15^\circ$. The P part is for the current controller set to 0.3, which gives the references to the inner loop controller: $0.3 \cdot 20 = 6^\circ$, $0.3 \cdot 40 = 12^\circ$. Hence the pitch reference will not be saturated and the controlled system should follow somewhat linear behaviour, i.e., double reference change = double control signal (Figure 5.4) but the same rise time.

It should also be pointed out that the depth change is in sledge mode, since the reference changes was greater than the threshold (Table 5.4). During the turn, the

[1] The authors learned this fact from a co-worker at SAAB who have attended SASS product testings

region	1	2	3
region	according to Figure 4.14	"	"
manoeuvring r_{ref}	true at reference change $> 1^\circ$, false when heading error < 1m and $r < 0.02$rad/s	"	"
manoeuvring θ_{ref}	-	turns off at a reference change > 3.5m, turns on when depth error < 3m and $\theta < 1^\circ$	turns off at a reference change > 3m turns on when depth error < 3m
sledge/ elevator mode	elevator mode	sledge mode if *manoeuvre*, else elevator mode	sledge mode
heave ctrl enabler	on	!*manoeuvre*	off
integrator enable for r	!*manoeuvre* & ctrl effort $r < 0.9$	"	"
integrator enable for ϕ	ctrl effort $\phi < 0.9$	"	"
integrator enable for θ	ctrl effort $\theta < 0.9$	!*manoeuvre* & ctrl effort $\theta < 0.9$	!*manoeuvre* & ctrl effort $\theta < 0.9$

Table 5.4: Switching conditions for the outer loop controller.

controller is in depth keeping, i.e., elevator mode, which is seen in Figure 5.4 where the heave controller is compensating the depth error during the turn.

Test Case Two

In this simulation the submarine will accelerate through all three velocity regions while given a reference change in depth. This will show how the control system handles the transfer between the different controllers. The results can be seen in Figures 5.5-5.8.

Depth change A reference change is ordered at T = 100s, at the same time the rotor RMS is increased and starts accelerating the submarine, see Figure 5.5. The velocity region changes are marked with red rings, and occurs according to Figure 4.14 around 6 and 13 knots, or approximately 3.2 and 7 m/s.

Figure 5.7 displays the pitch, which in the first region is kept low. Figure 5.8 shows that the bow plane heave effort is large, meaning that the submarine changes depth in an elevating fashion, as ordered by the outer controller.

In the second region, depth changing should be performed in a sledge fashion (Table 4.2), meaning that it should pitch to change depth. This is confirmed in Figure 5.7, where the submarine starts to pitch after the region change. Figure 5.8 shows how the aft and the tower hydroplanes work together to pitch the submarine. Worth pointing out is the acceleration of the depth change when entering the second region, i.e. changing from elevator mode to sledge mode. Depth changing seems to be slower in elevator mode.

In the top speed region depth should, according to Table 4.2, only be controlled by the stern hydroplanes. This means that the control effort from the bow planes should be zero, which can clearly be seen in Figure 5.8.

During the moments of the switches, bumps in the control efforts are distinguishable, i.e., an effect from the gain scheduling explained in Section 4.4. This is an undesirable behaviour, but fortunately, a manoeuvre like this is probably rare.

Test Case Three

Test case three will be similar to the previous one, except that the submarine will turn two full laps while accelerating, instead of diving. This will illustrate how the heading controller performs in the different regions. The results are shown in Figures 5.9-5.12.

Heading change As in the previous test case, the changes of regions are marked with red circles in the figures. According to Figures 5.9 and 5.10, the max speed at the final RPS of the propeller is apparently around 7.5 m/s when turning and 9 m/s when traveling straight.

Figure 5.11 contains an *xy* position graph relative to the initial position. Figure 5.12 shows the control efforts and Figure 5.10, shows the heading.

As for the control effort in Figure 5.12, the controller is more aggressive in the high speed region than in the low and medium speed regions. This is preferred since often when travelling at slow speed, the submarine should produce minimal noise.

In Figure 5.10, a noticeable increase in heading derivative takes place at the change between the low and medium velocity region, even though the control effort is about the same. According to Section 4.3 the forces from the hydroplanes depend on the velocity u squared, it is therefore expected that the submarine will turn faster at higher speeds.

It is worth pointing out that the roll and pitch efforts increase in magnitude as the speed gets higher. This is noted especially for the roll effort, where it is more than 50% of maximum control effort during T= 400-600s. Figure 5.13 displays zero roll. The controller is apparently compensating for huge hydrodynamic forces acting to roll the submarine. The turn is to starboard, and the roll effort says the rudders want to roll the submarine anti-clockwise seen from behind. Thus, the forces acting on the submarine during the turn seems to tend to roll the submarine inwards.

Rotor

This is just a brief Section of how the rotor RPS translates to the submarine velocity. As seen in Figure 5.14, the relation seems to be linear, or at least affine.

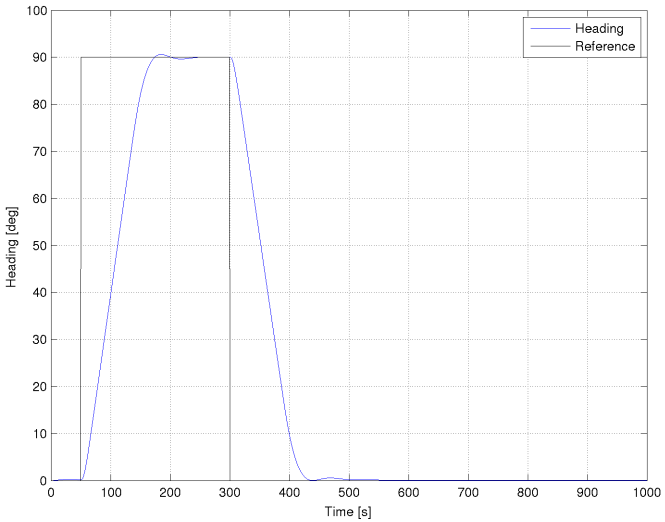

Figure 5.1: Test case one, Heading.

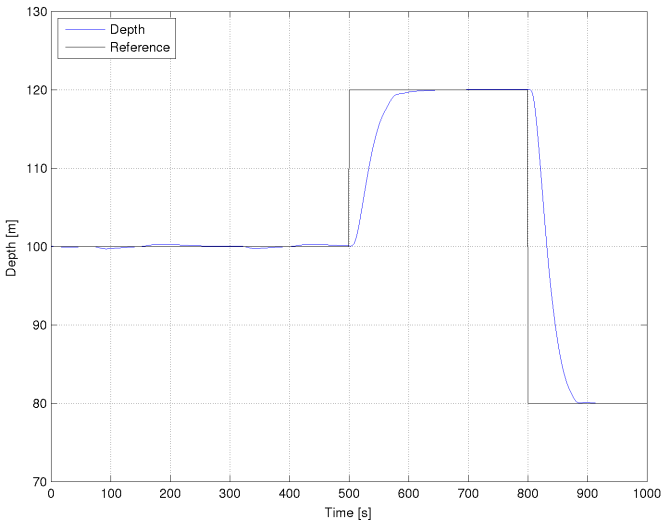

Figure 5.2: Test case one, Depth.

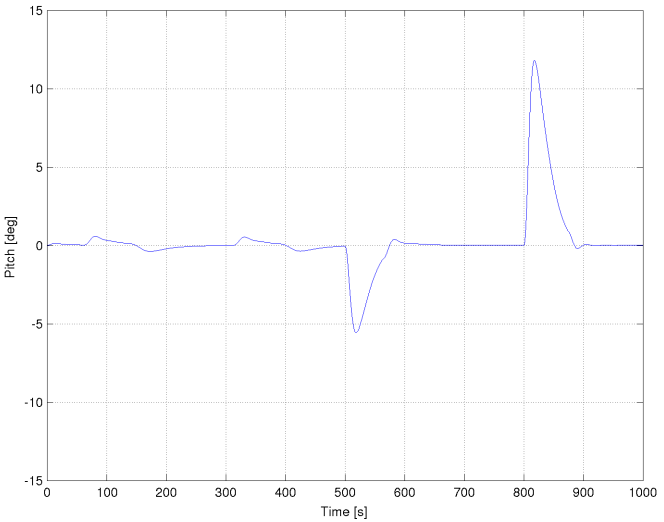

Figure 5.3: Test case one, Pitch.

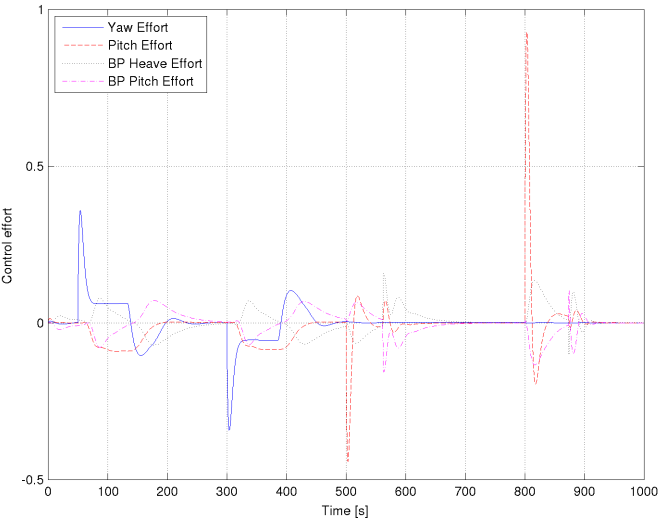

Figure 5.4: Test case one, Control Efforts.

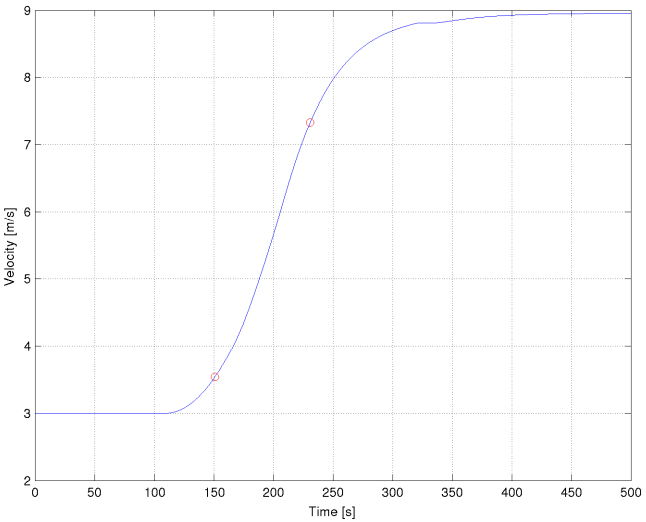

Figure 5.5: Test case two, Velocity.

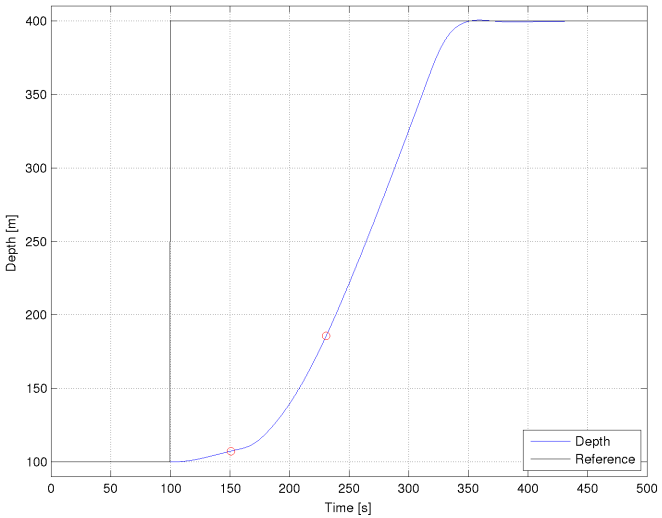

Figure 5.6: Test case two, Depth.

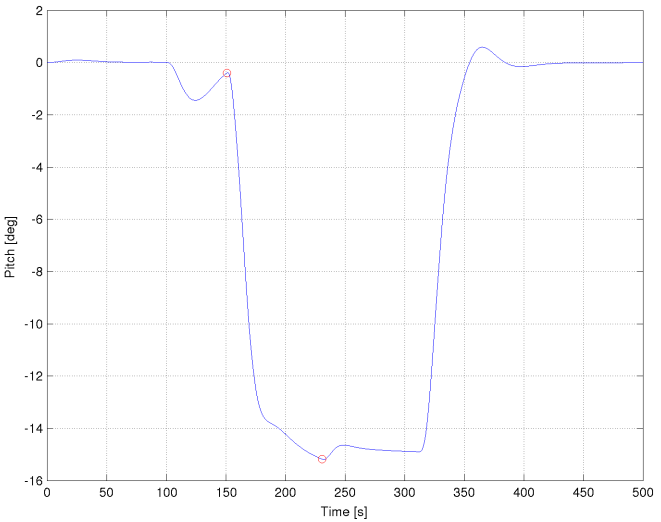

Figure 5.7: Test case two, Pitch.

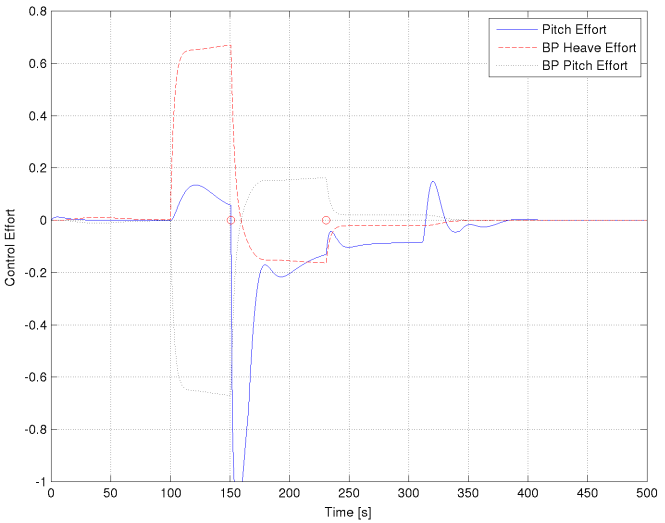

Figure 5.8: Test case two, Control Efforts.

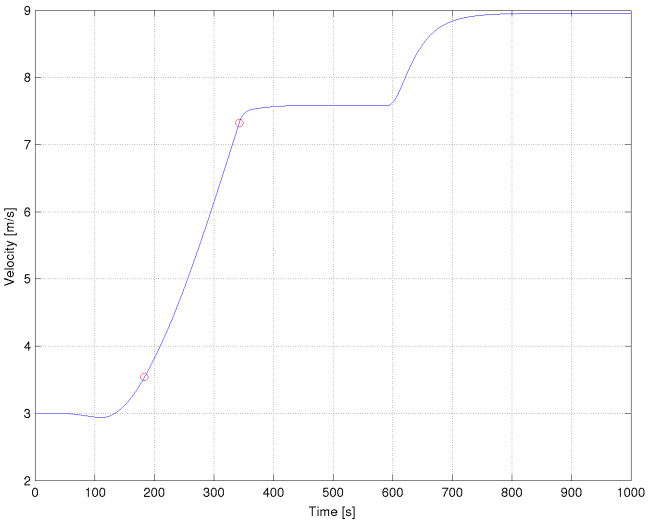

Figure 5.9: Test case three, Velocity.

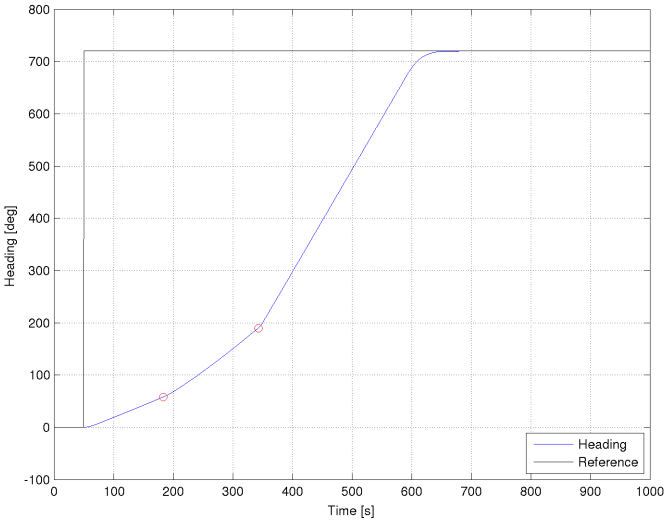

Figure 5.10: Test case three, Heading.

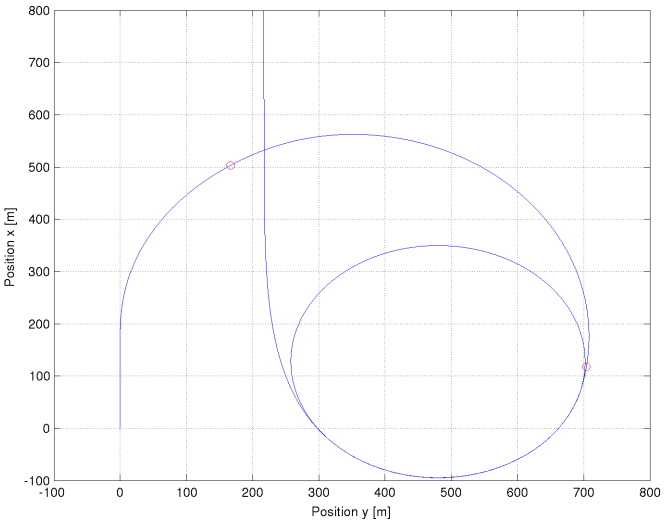

Figure 5.11: Test case three, Position in the xy-plane.

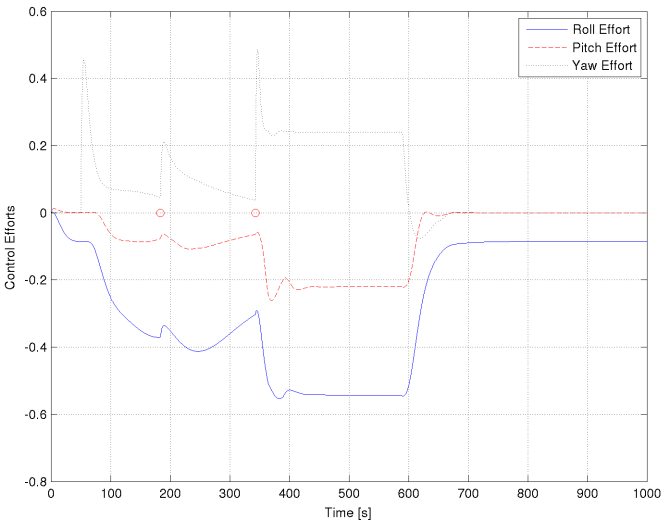

Figure 5.12: Test case three, Control Efforts.

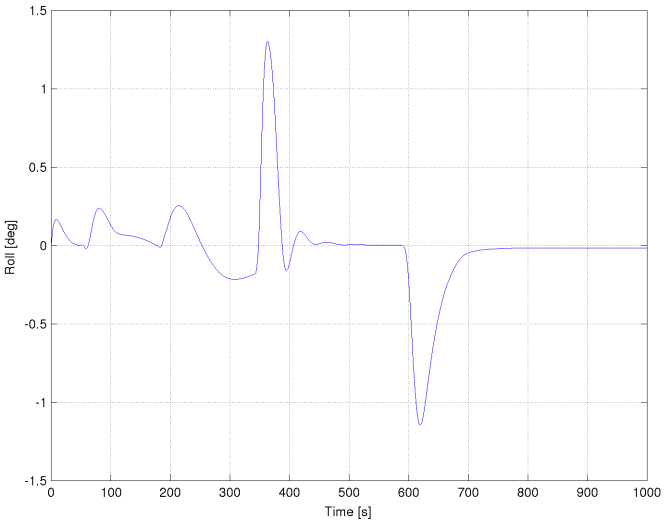

Figure 5.13: Test case three, roll.

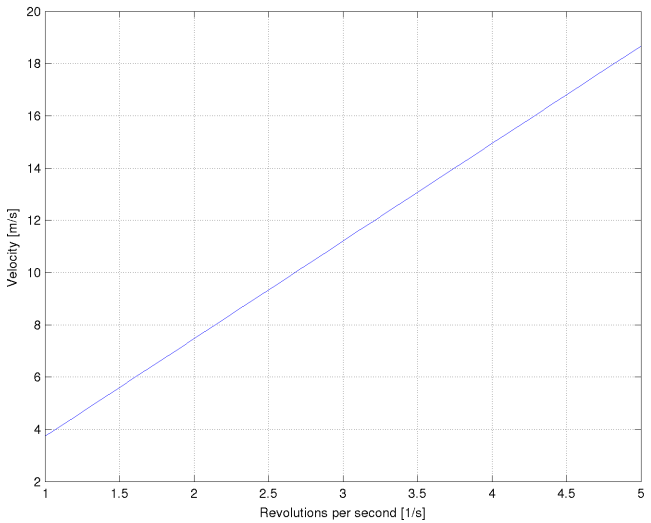

Figure 5.14: RPS of the rotor vs. velocity.

6

Discussion

6.1 Hydrodynamic Coefficients discussion

Hydrodynamic coefficients can be analytically approximated with empirical formulas according to [Humphreys and Watkinson, 1978]. This method was applied to the demo submarine received from FOI, and the results were compared with FOIs hydrodynamic coefficients. They are both presented and compared in Table 6.1. Some coefficients differ by up to 450%, however, it can be discussed how important accuracy is for these coefficients.

[Humphreys and Watkinson, 1978] claims that there are 15 coefficients that are more important than others. In Table 6.1, the error percentages between the approximated and received coefficients are calculated and presented in the right most column. Some of the coefficients with the highest error percentage are not among the 15 most important coefficients, however, the results are still differ by large values. This inaccuracy is probably the reason why this method is not commonly used, since model tests or advanced CFD calculations are much more accurate.

Table 6.1: Hydrodynamic coefficients, Measured vs. Calculated.

Coefficient	FOI Measured	Calculated	Difference (%)	Humphrey difference (%)
$X_{\dot{u}}$	$-5.8503 \cdot 10^4$	$-3.8999 \cdot 10^4$	33.33	11.5
$X_{u\|u\|}$	$-2.1638 \cdot 10^3$	$-1.0567 \cdot 10^4$	-388.35	-
X_{vv}	$2.2024 \cdot 10^4$	-	-	-
X_{vr}	$1.9609 \cdot 10^6$	$2.057 \cdot 10^6$	-4.9	8.0
X_{ww}	$7.2193 \cdot 10^3$	-	-	-
X_{wq}	$-1.4999 \cdot 10^6$	$-1.8898 \cdot 10^6$	-26	0.1
X_{pr}	$3.7801 \cdot 10^6$	$1.0718 \cdot 10^6$	71.65	-
X_{qq}	$6.0774 \cdot 10^6$	$-3.6633 \cdot 10^5$	106.03	-
X_{rr}	$8.5083 \cdot 10^6$	$1.7035 \cdot 10^6$	79.98	-
$Y_{\dot{v}}$	$-2.1199 \cdot 10^6$	$-2.0570 \cdot 10^6$	2.97	8.0
$Y_{\dot{p}}$	$-3.7801 \cdot 10^6$	$-1.0718 \cdot 10^6$	71.65	-
$Y_{\dot{r}}$	$-1.2619 \cdot 10^7$	$-1.7035 \cdot 10^6$	86.50	-
$Y_{v\|v\|}$	$-1.2348 \cdot 10^5$	-	-	-

Y_{uv}	$-1.1988 \cdot 10^5$	-	-	-
Y_{up}	$-1.5497 \cdot 10^5$	-	-	-
Y_{ur}	$1.0018 \cdot 10^5$	$-3.8999 \cdot 10^4$	138.93	-
Y_{wp}	$1.6215 \cdot 10^6$	$1.8898 \cdot 10^6$	-16.55	0.1
Y_{pq}	$1.5436 \cdot 10^6$	$3.6633 \cdot 10^5$	76.27	-
$Z_{\dot{w}}$	$-1.6215 \cdot 10^6$	$-1.8898 \cdot 10^6$	-16.55	0.1
$Z_{\dot{q}}$	$-1.5436 \cdot 10^6$	$-3.6633 \cdot 10^5$	76.27	65.0
Z_{uw}	$-4.6835 \cdot 10^4$	-	-	-
Z_{uq}	$-4.8830 \cdot 10^5$	$3.8999 \cdot 10^4$	107.99	-
Z_{vp}	$-2.1199 \cdot 10^6$	$-2.0570 \cdot 10^6$	2.97	8.1
Z_{pp}	-	$-1.0718 \cdot 10^6$	-	-
Z_{pr}	-	$-1.7035 \cdot 10^6$	-	-
Z_{ww}	$6.5568 \cdot 10^3$	-	-	-
$K_{\dot{v}}$	$-3.7801 \cdot 10^6$	$-1.0718 \cdot 10^6$	71.65	44.0
$K_{\dot{p}}$	$-1.3637 \cdot 10^7$	$-7.1006 \cdot 10^6$	47.93	93.0
$K_{\dot{r}}$	$-2.7968 \cdot 10^7$	$-1.4349 \cdot 10^7$	48.69	-
$K_{v\|v\|}$	$-8.8960 \cdot 10^5$	-	-	-
K_{uv}	$-4.3689 \cdot 10^5$	-	-	-
K_{up}	$-5.0448 \cdot 10^6$	-	-	-
K_{ur}	$-5.6544 \cdot 10^6$	-	-	-
K_{vw}	-	$1.6722 \cdot 10^6$	-	-
K_{vq}	-	$-2.0698 \cdot 10^6$	-	-
K_{wp}	$3.7801 \cdot 10^6$	$1.0719 \cdot 10^6$	71.64	-
K_{wr}	-	$2.0698 \cdot 10^6$	-	-
K_{qr}	$-7.5 \cdot 10^7$	$-3.33 \cdot 10^7$	55.6	-
$M_{\dot{w}}$	$-4.2177 \cdot 10^6$	$-3.6633 \cdot 10^5$	91.31	64.0
$M_{\dot{q}}$	$-3.9850 \cdot 10^8$	$-3.6229 \cdot 10^8$	9.09	10.0
$M_{w\|w\|}$	$-4.4401 \cdot 10^5$	-	-	-
M_{uw}	$5.4147 \cdot 10^5$	$5.5523 \cdot 10^5$	-2.54	-
M_{uq}	$-2.3875 \cdot 10^7$	$1.8898 \cdot 10^6$	107.92	-
M_{vp}	-	$1.7035 \cdot 10^6$	-	-
M_{vr}	-	$-1.0718 \cdot 10^6$	-	-
M_{pp}	-	$1.4349 \cdot 10^7$	-	-
M_{pr}	$4.5986 \cdot 10^8$	$3.8849 \cdot 10^8$	15.52	11.4
M_{rr}	-	$1.4349 \cdot 10^7$	-	-
$N_{\dot{v}}$	$4.8619 \cdot 10^5$	$-1.7035 \cdot 10^6$	450.38	-
$N_{\dot{p}}$	$-2.7968 \cdot 10^7$	$-1.4349 \cdot 10^7$	48.69	-
$N_{\dot{r}}$	$-4.7351 \cdot 10^8$	$-3.9559 \cdot 10^8$	16.46	10.7
$N_{v\|v\|}$	$9.7812 \cdot 10^5$	-	-	-
N_{uv}	$-2.2747 \cdot 10^6$	$-2.0180 \cdot 10^6$	11.29	-
N_{up}	$-1.6776 \cdot 10^6$	$-1.0718 \cdot 10^6$	36.11	-
N_{ur}	$-3.4493 \cdot 10^7$	$-1.7035 \cdot 10^6$	95.06	-
N_{vq}	-	$1.0718 \cdot 10^6$	-	-
N_{wp}	-	$-3.6633 \cdot 10^5$	-	-
N_{pq}	$-3.8486 \cdot 10^8$	$-3.5519 \cdot 10^8$	7.71	10.7

N_{qr}	-	$1.4349 \cdot 10^7$	-	-

6.2 Linearised state space model

A total of three linear state space system were derived in this thesis. A short discussion of the third model, i.e., the high velocity region, is presented here. The model itself is presented in Figure 6.1. Some parts of the state space system is what can be expected. The hydroplanes follow a first order characteristics with time constant $T = 3$. The system was linearised with no roll/pitch, hence ϕ and θ are the integrals of p and q. As for the u characteristics, rudder angles δ_1, δ_2, δ_5 and δ_6 give a positive addition to $\dot{u}$. This appear as strange at a first glance, and the Coriolis effect from the six degrees of freedom dynamics is most likely the source of this.

How rudder angles influence the acceleration, e.g., $\dot{r}$, differs between the rudders. This does also seem strange and is most likely also caused by the Coriolis effect.

6.3 Controller issues

The control system contains numerous numbers of nonlinearities in forms of saturations and logical switches, especially in the outer loop. Nonlinearities in the loop can be a source of possible oscillations. These can be difficult to locate, but in this section a few possible origins for oscillations and other controller problems will be discussed.

Sledge mode depth control

Depth control in sledge mode is performed by a P controller in cascade with an inner loop state feedback/feedforward controller with an integrated I part. The I part is disabled at the moment of a reference change and reenabled when the control error is less than 3m and the pitch is less then 1°, see Table 5.4. The reason to include an I part is to remove stationary errors, but a stationary error greater than 3 meters from the reference point will not enable the I part, hence, continue to exist.

Since the pitch has to be less then 1° to enable the I part, this could be a source of oscillations around a reference depth.

These effects have at this point not yet shown up. Either do they not exist at all, or perhaps only appear at special cases. Introducing disturbances could perhaps also make these effects show up.

Course control

Analogous with the sledge depth control, the course control could experience the same problems, although, has not at this point.

```
a =
              phi     theta        d1        d2        d3        d4        d5        d6         u         v         w         p         q         r
   phi          0         0         0         0         0         0         0         0         0         0         0         1         0         0
   theta        0         0         0         0         0         0         0         0         0         0         0         0         1         0
   d1           0         0   -0.3333         0         0         0         0         0         0         0         0         0         0         0
   d2           0         0         0   -0.3333         0         0         0         0         0         0         0         0         0         0
   d3           0         0         0         0   -0.3333         0         0         0         0         0         0         0         0         0
   d4           0         0         0         0         0   -0.3333         0         0         0         0         0         0         0         0
   d5           0         0         0         0         0         0   -0.3333         0         0         0         0         0         0         0
   d6           0         0         0         0         0         0         0   -0.3333         0         0         0         0         0         0
   u     3.778e-08 -0.003094  0.002602  0.002602 -0.002602 -0.002602  0.002968  0.002969 -0.02495  2.279e-08  0.004304  4.261e-07 -0.1846  3.012e-07
   v       0.4033  5.953e-07 -0.003928 -0.1031  -0.1031  -0.002927 -5.632e-07 -5.632e-07  0.009468  0.1061  -8.164e-07 -44.317  3.515e-05  0.694
   w     -4.574e-08  0.003747  0.02597   0.02597  -0.02597  -0.02597  -0.07411  -0.07411  1.940e-05 -2.761e-08 -0.1103  -5.159e-07  3.487  -3.649e-07
   p     -1.054e-07 -0.00865   0.05428   0.05204   0.05204   0.05428   0         0        -4.701e-05  6.371e-08  0.01203   1.191e-06 -0.516   8.423e-07
   q      1.054e-07  0         -0.003725  0.002725  -0.002725  -0.002725  0.008298  0.008298  4.496e-05 -6.171e-08  0.01203   1.191e-06 -0.516   8.423e-07
   r      0.02628   0         -0.009568  0.002592  0.002592  -0.009568  0         0         6.159e-05 -0.02401  0         0.2569    0         -0.3955

b =
              d1        d2        d3        d4        d5        d6
   phi         0         0         0         0         0         0
   theta       0         0         0         0         0         0
   d1     0.3333         0         0         0         0         0
   d2          0    0.3333         0         0         0         0
   d3          0         0    0.3333         0         0         0
   d4          0         0         0    0.3333         0         0
   d5          0         0         0         0    0.3333         0
   d6          0         0         0         0         0    0.3333
   u           0         0         0         0         0         0
   v           0         0         0         0         0         0
   w           0         0         0         0         0         0
   p           0         0         0         0         0         0
   q           0         0         0         0         0         0
   r           0         0         0         0         0         0

c =
                phi     theta        d1        d2        d3        d4        d5        d6         u         v         w         p         q         r
   Demux/r        0         0         0         0         0         0         0         0         0         0         0         0         0         1
   Demux1/roll    1         0         0         0         0         0         0         0         0         0         0         0         0         0
   Demux1/pitch   0         1         0         0         0         0         0         0         0         0         0         0         0         0

d =
                d1  d2  d3  d4  d5  d6
   Demux/r       0   0   0   0   0   0
   Demux1/roll   0   0   0   0   0   0
   Demux1/pitch  0   0   0   0   0   0
```

Figure 6.1: Linear model in the high velocity region.

Overly complicated controller

The final control structure can feel a bit overambitious. The controller could have been simplified by adding PID controllers in the r,ϕ and θ directions. This would remove the state FF, FB and the observer part and turn the I parts controller into PIDs. *Hopefully*, however, this would result in a poorer performing controller but with increased simplification.

An LQ controller relies on the state space model to be relatively accurate. If the controller presented in this thesis would be implemented in a real submarine and turn out to be inadequate, tuning it, is not straightforward since it requires tuning of the model itself. A PID however, is simpler to tune on spot. The PIDs in the submarine could, e.g., be based on a PID design derived in the lab, and then tuned by changing the P, I, and D gains[1].

6.4 Future Work

This master thesis is only the start of a project that could be developed much further. This means that there are lots of room for future work and improvements.

Model

Sensor Models Measured values from sensors always come with an uncertainty. Adding noise to measured signals in the submarine simulator, is a step closer to test how the controller will perform in an actual vessel.

On a submarine, some sensor errors will differ depending on where the sensor is placed. For example, the velocity sensor is often a pressure sensor placed on the submarine hull. If the flow around the hull is turbulent, this could cause large noise levels to the log.

The water pressure due to the suppressed water by the submarine bow can also change over the hull. Multiple pressure sensors placed at different locations are therefor often used. The measured log velocity is then a function of measured values from each sensor.

In Section 3.1, the added mass effect was explained, i.e., the water closest to the hull travels with the submarine, hence, increasing the apparent mass. This could be another source of a velocity log sensor inaccuracy. The sensor could measure the submarine's velocity relative the water closest to the hull, which is lower then the velocity relative the unaffected water, further away from the hull.

Currently, the measured depth is the depth of the submarine-fixed frame's origin. It can be discussed if this is the actual depth of the submarine. Perhaps the submarine's depth is the part of the submarine, that is deepest, which could be preferred when manoeuvring close to the seabed.

[1] There are more complex PID designs than the one presented in this thesis. A more complex PID design could include additional tuning parameters.

Tank System A submarine includes a number of different tanks which are used to control whether to sink or float, as well as the attitude of the submarine. Adding the tanks as possible actuators is a step closer to a perfect submarine simulator.

A simple way to model the effects from the tanks, is the possibility to affect the position of the center of gravity, and the weight of the submarine. A more accurate model of the tank system, could be to model the pump dynamics as well as the flow characteristics in the tanks and tubes.

Additional Hydrodynamic Effects There are more hydrodynamic effects that need to be taken into account for a complete simulator system. Among them are different effects that occur near the surface or near the bottom.

At the moment, it is only possible to specify a linear current in a specific direction in the simulation. It might be useful, to also be able to simulate irregular currents and turbulence, to see how the controller handles these conditions, since it is closer to the reality.

Simulating Alarms An important duty of the SASS, is error detection and alarm presentation. This indicates to the helmsman if anything has malfunctioned on the submarine, for example a hydroplane angle fault or pump malfunction. It would therefore be useful to be able to simulate these alarms, and present them to the user of the simulator system. These errors should also be sent to the autopilot, if, for example, a hydroplane is not responding, the autopilot should take this into account when steering the submarine.

Implementation

The focus of the thesis have been mostly on physical modelling and controller design, and less on the program for target system, i.e., the test rig. This means that there is a lot of room for improvement here, especially within usability.

User Interface The test rig has a software version of a hardware console in a submarine. The original goal was to implement the simulator system with the interface, but due to the unexpected complexity of hydrodynamic modelling, this was postponed as a future project.

At the moment, the simulator system is communicated with through the terminal in Linux. A sensor value or a new reference, has to be explicitly requested by a terminal command. This is not a user friendly setup, which is the reason why the simulator system needs to be implemented with the test rig user interface in order to properly benefit from the submarine simulator.

In a far future, it might also be desirable to implement compatibility with existing hardware from a submarine, to be able to train personnel on land.

Animation A simple animation of the submarine attitude and hydroplane position was developed in Simulink. A picture of the animations can be found in Figure 6.2. At the moment, the animations are only available when simulating the submarine in Simulink, and not when running the simulator on the target system, hence, a desired

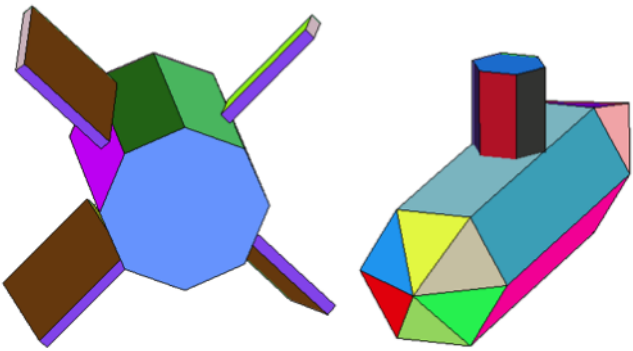

Figure 6.2: Rudder and submarine attitude animation.

feature could be to implement a TCP communication with the animations and the submarine simulator.

Bibliography

ActiveState. *Tool command language*. URL: http://www.tcl.tk/ (visited on 07/08/2014).

Åström, K. J. and C. G. Källström (1976). *Identification of ship steering Dynamics*. Tech. rep.

Feldman (1979). *DTNSRDC Revised standard submarine equations of motion*. Tech. rep. Carderock Division of the Naval Surface Warfare Center, Maryland, USA.

Fossen, T. (2011). *Marine Craft Hydrodynamics and Motion Control*. John Wiley Sons Ltd.

Fossen, T. I. (1994). *Guidance and Control of Ocean Vehicles*. John Wiley Sons Ltd.

Fossen, T. I. and O.-E. Fjellstad (1995). *Nonlinear Modeling of Marine Vehicles in 6 Degrees of Freedom*. Tech. rep. The Norwegian Institude of Technology, Trondheim, Norway.

Glad, T. and L. Ljung (2003). *Reglerteori*. Studentlitteratur AB Lund.

Hickey, R. I. (1990). *Submarine motion simulation including zero forward speed and propeller race effects*. Tech. rep. MIT, Department of Ocean Engineering, Massachusetts, USA.

Humphreys and Watkinson (1978). *Prediction of acceleration hydrodynamic coefficients for underwater vehicles from geometric parameters*. Tech. rep. Naval Coastal System Laboratory, Florida, USA.

Lamb, S. H. (1932). *Hydrodynamics*. University Press, New York, USA.

Larsson, L. and H. Raven (2010). *Ship resistance and flow*. The society of Naval Architects and Marine Engineers.

Mathworks. *Matlab*. URL: http://www.mathworks.se/products/matlab/ (visited on 07/08/2014).

Mathworks. *Simulink*. URL: http://www.mathworks.se/products/simulink/ (visited on 07/08/2014).

Ridley, P., J. Fontan, and P. Corke (2003). *Submarine Dynamic Modeling*. Tech. rep. Queensland University of Technology, Queensland, Australia.

Toxopeus (2011). *Practical application of viscous-flow calculations for the simulation of manoeuvring ships*. PhD thesis. Maritime Reasearch Institute Netherlands.

Watt (2007). *Modelling and Simulating Unsteady Six Degrees-of-Freedom Submarine Rising Maneuvers*. Tech. rep. Defence Research and Development Canada, Atlantic, Canada.

A

Appendix

A.1 K_t and K_q interpolation polynomials

Equations for K_T and K_Q:

$$\begin{aligned} K_T(J) =& 0.410758 - 0.115654J - 0.107836J^2 + 0.0713369J^3 \\ & - 0.00620451J^4 - 0.0127538J^5 + 0.00487893J^6 \\ & - 0.000678484J^7 + 0.0000333463J^8 \end{aligned} \tag{A.1}$$

$$\begin{aligned} K_Q(J) =& 0.0690631 - 0.0249658J - 0.00623472J^2 \\ & + 0.00171807J^3 + 0.00579169J^4 - 0.00559630J^5 \\ & + 0.00178950J^6 - 0.000246886J^7 + 0.0000126029J^8 \end{aligned} \tag{A.2}$$

Lund University
Department of Automatic Control
Box 118
SE-221 00 Lund Sweden

Document name
MASTER´S THESIS

Date of issue
September 2014

Document Number
ISRN LUTFD2/TFRT--5954--SE

Author(s)
Erik Lind
Magnus Meijer

Supervisor
Hans Bohlin, Saab
Karl-Erik Årzén, Dept. of Automatic Control, Lund University, Sweden (examiner)

Sponsoring organization

Title and subtitle
Simulation and Control of Submarines

Abstract

When designing control systems for real applications, it is important to first do testing in a simulated environment, to ensure adequate performance. This is especially important when designing control systems for applications that have high operation costs, e.g., submarines, since late errors in the development can be extremely costly.

Saab develops steering systems for submarines. Prior to this thesis, testing for those have been performed in an open-loop environment, where only static test cases could be examined. Saab therefore identified the need to implement a dynamic test simulator, which could react to the different signals from the steering system, i.e., act as a real submarine.

In this thesis, such a simulator was developed. It consists of two parts, a physical model of a submarine, and a control system for motion control. As for the physical submarine model, it can be approximated from mechanical data of a submarine that the user provide, such as dimensions and weight. The second options is for the user to explicitly supply the simulator with hydrodynamic coefficients.

The control system was derived to control a model of a demo submarine. Saab is also involved in submarine navigation systems and saw the need to, in the future, also have the possibility to test those products. A navigation system assumes an autopilot exists, hence, an autopilot control system was developed.

In the end, the control system consisted of a two-level cascade controller of mixed LQG- and PID-control, along with a Kalman estimator for estimating unknown states.

The results were overall satisfactory. The performance of the control system is well within usual customer specifications and the main problems in this thesis lay in getting a proper model.

Keywords

Classification system and/or index terms (if any)

Supplementary bibliographical information

ISSN and key title
0280-5316

ISBN

Language
English

Number of pages
1-87

Recipient's notes

Security classification

http://www.control.lth.se/publications/